

AD-A055 283

IIT RESEARCH INST ANNAPOLIS MD
ANALYSIS OF RECEIVER MIXERS.(U)
MAR 78 M A MAIUZZO

F/G 9/4

F19628-78-C-0006
NL

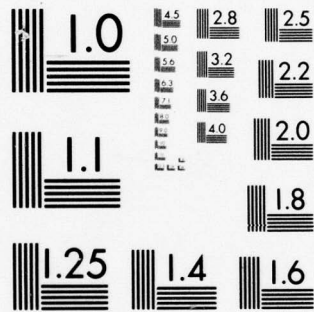
ESD-TR-78-100

UNCLASSIFIED

| of |
AD
A055283



END
DATE
FILMED
7 -78
DDC



MICROCOPY RESOLUTION TEST CHART
NATIONAL BUREAU OF STANDARDS-1963-A

FOR FURTHER TRAN ~~SM 11~~

ESD-TR-78-100

12

[Handwritten signature]

AD A 055283

ANALYSIS OF RECEIVER MIXERS

IIT Research Institute
Under Contract to
DEPARTMENT OF DEFENSE
Electromagnetic Compatibility Analysis Center
Annapolis, Maryland 21402

175 300



March 1978

FINAL REPORT

DDDC
JUN 19 1978
[Handwritten signature]

Approved for public release; distribution unlimited.

AD No.
DDC FILE COPY

78 06 09 053

ESD-TR-78-100

This report was prepared by the IIT Research Institute under Contract F-19628-78-C-0006 with the Electronic Systems Division of the Air Force Systems Command for the technical operation of the DoD Electromagnetic Compatibility Analysis Center, Annapolis, Maryland.

This report has been reviewed and is approved for publication.

Michael Maiuzzo

MICHAEL A. MAIUZZO
Project Engineer, IITRI

R. B. Warren

R. B. WARREN
Assistant Director
Contractor Operations

Approved by:

Thomas A. Anderson

THOMAS A. ANDERSON
Colonel, USAF
Director

A. M. Messer

A. M. MESSER
Chief, Plans & Resource
Management Office

UNCLASSIFIED

SECURITY CLASSIFICATION OF THIS PAGE (When Data Entered)

9 REPORT DOCUMENTATION PAGE		READ INSTRUCTIONS BEFORE COMPLETING FORM	
1. REPORT NUMBER 18 ESD-TR-78-100	2. GOVT ACCESSION NO.	3. RECIPIENT'S CATALOG NUMBER	
4. TITLE (and Subtitle) 6 ANALYSIS OF RECEIVER MIXERS.		5. TYPE OF REPORT & PERIOD COVERED 9 FINAL rept.	
7. AUTHOR(s) 10 Michael A. Maiuzzo		8. CONTRACT OR GRANT NUMBER(s) 15 F-19628-78-C-0006	
9. PERFORMING ORGANIZATION NAME AND ADDRESS		10. PROGRAM ELEMENT, PROJECT, TASK AREA & WORK UNIT NUMBERS	
11. CONTROLLING OFFICE NAME AND ADDRESS		12. REPORT DATE 11 March 1978	
		13. NUMBER OF PAGES 78 12 73p.	
14. MONITORING AGENCY NAME & ADDRESS (if different from Controlling Office)		15. SECURITY CLASS. (of this report) UNCLASSIFIED	
		15a. DECLASSIFICATION/DOWNGRADING SCHEDULE	
16. DISTRIBUTION STATEMENT (of this Report) Approved for public release; distribution unlimited.			
17. DISTRIBUTION STATEMENT (of the abstract entered in Block 20, if different from Report)			
18. SUPPLEMENTARY NOTES UNLIMITED			
19. KEY WORDS (Continue on reverse side if necessary and identify by block number) DEMODULATOR NONLINEAR INTERMODULATION MATHEMATICAL MODEL MIXER MEASURED DATA SPURIOUS RESPONSE			
20. ABSTRACT (Continue on reverse side if necessary and identify by block number) Procedures are presented for estimating desired and undesired receiver mixer responses. Computer models, developed using the Taylor-Fourier series method to analyze double-balanced-diode and single-diode mixers, are described.			

DDDC
JUN 19 1978
RECEIVED
F

78 06 09 053

act

PREFACE

The Electromagnetic Compatibility Analysis Center (ECAC) is a Department of Defense facility, established to provide advice and assistance on electromagnetic compatibility matters to the Secretary of Defense, the Joint Chiefs of Staff, the military departments and other DoD components. The center, located at North Severn, Annapolis, Maryland 21402, is under the policy control of the Assistant Secretary of Defense for Communication, Command, Control, and Intelligence and the Chairman, Joint Chiefs of Staff, or their designees, who jointly provide policy guidance, assign projects, and establish priorities. ECAC functions under the executive direction of the Secretary of the Air Force and the management and technical direction of the Center are provided by military and civil service personnel. The technical operations function is provided through an Air Force-sponsored contract with the IIT Research Institute (IITRI).

This report was prepared as part of AF Project 649E under Contract F-19628-78-C-0006 by the staff of the IIT Research Institute at the Department of Defense Electromagnetic Compatibility Analysis Center.

To the extent possible, all abbreviations and symbols used in this report are taken from American Standard Y10.19 (1967) "Units Used in Electrical Science and Electrical Engineering" issued by the USA Standards Institute.

Users of this report are invited to submit comments that would be useful in revising or adding to this material to the Director, ECAC, North Severn, Annapolis, Maryland 21402, Attention XM.

ACCESSION for	
NTIS	<input checked="" type="checkbox"/> NTIS Section
DDC	<input type="checkbox"/> DDC Section
UNCLASSIFIED	<input type="checkbox"/>
CLASSIFIED	
BY	DISTRIBUTION/AVAILABILITY CODES
DI	SPECIAL
<i>A</i>	

EXECUTIVE SUMMARY

Computer models, developed using the Taylor-Fourier series method to analyze double-balanced-diode and single-diode mixers, are described. Use of this method results in mixer models that are considerably different in form than those obtained by past methods; the predicted response levels are in close agreement with measured data. These models were developed by the Electromagnetic Compatibility Analysis Center (ECAC) to provide improved procedures for estimating desired and undesired receiver responses due to the nonlinearity of the mixer. These undesired responses may include cross modulation, intermodulation, spurious responses and desensitization.

The models are used to compute nonlinear response amplitudes based on the nominal values of resistors, inductors, and capacitors in the circuit, the local oscillator voltages, and the direct current (dc) characteristic of the diode(s). Measured spurious responses were compared with spurious responses calculated by the models and were in close agreement.

Procedures for developing additional mixer models are also described.

The methods described herein and the measured intermodulation data normally acquired for equipment in obtaining a spectrum signature can be used to make reasonable estimates of levels of many other intermodulation responses. These other responses can be significant in an electromagnetic compatibility analysis, but are not measured.

TABLE OF CONTENTS

<u>Subsection</u>	<u>Page</u>
SECTION 1	
INTRODUCTION	
BACKGROUND	1
OBJECTIVE	2
APPROACH	2
SECTION 2	
THE POWER SERIES MIXER MODEL	
POWER SERIES ANALYSIS FOR A DIODE MIXER	5
AN ILLUSTRATIVE EXAMPLE OF POWER SERIES LIMITATION	9
SECTION 3	
TAYLOR-FOURIER SERIES MIXER MODEL	
BACKGROUND	11
THE TAYLOR-FOURIER METHOD	11
USING THE RESPONSE COEFFICIENTS, $a_{p,Q}$	12
CALCULATING THE RESPONSE COEFFICIENTS	15
FREQUENCY-DEPENDENT RESPONSE COEFFICIENTS	22

TABLE OF CONTENTS (Continued)

<u>Subsection</u>	<u>Page</u>
SECTION 4	
RESULTS OF TAYLOR-FOURIER MODELING	
SINGLE-DIODE MIXERS (SDM)	23
DOUBLE-BALANCED-DIODE MIXERS (DBDM)	25
DBDM Predicted Responses	25
DBDM Parameter Sensitivity Study	25
A Perfectly Balanced DBDM	28
SECTION 5	
POWER SERIES COMPARED WITH TAYLOR-FOURIER SERIES	33
SECTION 6	
CONCLUSIONS	35
LIST OF ILLUSTRATIONS	

Figure

1	Diode mixer circuit	6
2	For diode mixer power series coefficients normalized to second-order coefficient, in dB	7

TABLE OF CONTENTS (Continued)
 LIST OF ILLUSTRATIONS (Continued)

<u>Figure</u>		<u>Page</u>
3	Diode mixer current versus voltage characteristic	8
4	Ebers-Moll diode model	16
5	SDM circuit.	17
6	Modeled DBDM circuit	18
7	Measured and predicted spurious response values for SDM	24

LIST OF TABLES

<u>Table</u>		
1	MEASURED SPURIOUS RESPONSE LEVELS FOR HEWLITT-PACKARD HP10534a DOUBLE-BALANCED MIXER . . .	26
2	MEASURED SPURIOUS RESPONSE LEVELS FOR HEWLITT-PACKARD HP10514a DOUBLE-BALANCED MIXER . . .	27
3	PREDICTED SPURIOUS RESPONSE LEVELS FOR HEWLITT-PACKARD HP10534a DBDM	29
4	PREDICTED SPURIOUS RESPONSE LEVELS FOR HEWLITT-PACKARD HP10534a DBDM, WITH α_2 INCREASED BY 5 VOLTS. ⁻¹	30
5	HYPOTHETICAL PERFECTLY BALANCED DBDM RESPONSES.	31

LIST OF APPENDIXES

<u>Appendix</u>		
A	COSAM REQUIREMENTS FOR INCLUSION OF ADDITIONAL INTERMODULATION (IM) PRODUCTS	37

TABLE OF CONTENTS (Continued)

LIST OF APPENDIXES (Continued)

<u>Appendix</u>	<u>Page</u>
B APPLYING MIXER SR REJECTION VALUES TO RECEIVER REJECTION CALCULATIONS	45
C "A COMPUTER PROGRAM FOR THE PREDICTION OF DIODE MIXER SPURIOUS RESPONSE LEVELS FOR CONDITIONS INCLUDING LARGE LOCAL OSCILLATOR LEVELS"	49
D CALCULATING DIODE PARAMETERS	55
E NUMERICAL SOLUTION FOR DOUBLE-BALANCED-DIODE MIXER CURRENTS	61
F THE C^Q EXPRESSIONS	63
G POWER SERIES DIVERGENCE FOR VACUUM TUBES. . .	67

SECTION 1
INTRODUCTION

BACKGROUND

Frequently, EMC analyses require estimation of the effects of nonlinear interactions. Equipment proximity and the resulting high interfering power levels on platforms such as airplanes, ships, and satellites, and in tactical environments, may produce the following nonlinear interactions:

1. Cross modulation
2. Receiver intermodulation (RIM)
3. Spurious responses (SR)
4. Desensitization
5. Transmitter intermodulation (TIM).

Estimates are sometimes based on measured data taken on a small sample of equipments of the same or similar design. However, because of the limited scope and increasing costs of most measured data, computerized equipment models are becoming more prevalent.

In the past, a major stumbling block in the development of accurate nonlinear-interaction receiver models has been the modeling of the mixer,¹ in many cases because of a basic flaw in the modeling method. A commonly used method can be described as follows. The current-voltage transfer

¹Donaldson, Jr., E. E. and Moss, R. W., *Study of Receiver Mixer Characteristics, Final Report*, Technical Report ECOM-01426-F, USAEC, Fort Monmouth, NJ, September 1966.

characteristic is represented by a power series; the input to the mixer is the sum of the radio-frequency (RF) and local oscillator (LO) signals. For practical mixer design, a flaw exists because the LO level is so high that either the series does not converge or the required number of terms becomes prohibitive (see Section 2 and APPENDIX G).

OBJECTIVE

The objective of this analysis was to present improved procedures for estimating receiver responses resulting from mixer nonlinearities.

APPROACH

A literature search was conducted for available mixer analysis methods. Most of the methods found were either not applicable to common mixer circuits or were not validated. One of the nonvalidated methods^{2,3} that appeared promising was selected for validation.

This method, which uses the Taylor-Fourier Series mixer model, is described in Section 3. It is used to calculate the magnitudes of response coefficients of a mixer. These response coefficients may be used to estimate the levels of the mixer's desired and undesired responses (i.e., spurious responses, intermodulation responses).

A 5-step method was used for developing the Taylor-Fourier series model for mixers and is presented in Section 3. Mixers are modeled as memoryless, voltage-dependent, current sources. The steps were as follows.

²Ehrman, L. and Graham, J. eds., *Nonlinear System Modeling and Analysis with Applications to Communications Receivers*, RADC-TR-73-178, USAF Rome Air Development Center, Rome, NY, June 1973.

³Terman, F. E., *Electronic and Radio Engineering*, McGraw-Hill, 4th Ed., New York, NY, 1955. Pp 573-575.

1. Model the current versus voltage characteristic of the nonlinear device.
2. Write the loop or node equations for the circuit.
3. Derive the expressions for the derivatives of the load current with respect to the RF source voltage. (A numerical procedure could be employed.)
4. Derive the expressions for the Taylor series coefficients as time variables.
5. Calculate the Taylor-Fourier series coefficients from a Fourier series expansion of each Taylor series coefficient.

Computer routines based on the 5-step method were then written and programmed. The computer routines were exercised to determine the theoretical response coefficient levels for a single-diode mixer (SDM) and a Hewlett Packard double-balanced-diode mixer (DBDM) circuit.

To help validate the Taylor-Fourier Series mixer models, measurements were made at ECAC of the mixer spurious responses resulting from the SDM and the DBDM circuits. Comparisons of the model predictions and the measured data were performed and are presented in Section 4 and APPENDIX C.

Procedures for calculating the receiver spurious response rejection on the basis of the mixer spurious-response coefficients are described in APPENDIX B.

A procedure for estimating certain high-order RIM coefficients on the basis of measured values of low-order RIM coefficients is described in APPENDIX A. The rationale for this extrapolation is based on the results of mixer performance predictions utilizing the Fourier-Series model.

Finally, a comparison of the modeling differences between the constant coefficient power series and the Taylor-Fourier Series is presented in Section 5.

SECTION 2

THE POWER SERIES MIXER MODEL

The power series analysis technique has been used to describe the spurious and intermodulation response characteristics of a mixer. The results are considerably different (Section 5) from those obtained by the Taylor-Fourier series analysis technique, as described in Section 3. As indicated below, the power series is not adequate when applied to a practical mixer design. The reason for this is that the power series coefficients are not constant with time due to the fact that the LO level is so large in practice that the "operating point level" (i.e., where the derivatives are evaluated) changes significantly over the time of one period of the LO waveform. Yet in a power series analysis, the coefficients are used as time-constant values. The Taylor-Fourier series takes the time variation into account by expanding each Taylor (or power) series coefficient in a Fourier series.

POWER SERIES ANALYSIS FOR A DIODE MIXER

Diode mixer circuits (Figure 1) have been analyzed in other reports and publications (see References 1, 4, and 5). Those results are useful for the purposes of this discussion. The relationship between the voltage (v) and the current (i) is given using:⁶

$$i = i_0 \left[e^{\alpha(v - iR_T)} - 1 \right] \quad (1)$$

⁴Steiner, J. W., "An Analysis of Radio Frequency in Interference Due to Mixer Intermodulation Products," *IEEE Transactions on EMC*, Vol. EMC-6, No. 1, January 1964.

⁵Herishen, J. T., "Diode Mixer Coefficients for Spurious Response Prediction," *IEEE Transactions on EMC*, Vol. EMC-10, No. 4, December 1968.

⁶Ebers J. J. and Moll, J. L., "Large-Signal Behavior of Junction Transistors," *Proceedings of the IRE*, December 1954.

where

- i_o = reverse leakage current, a constant, in amperes
 R_T = the total series circuit resistance, including the diode bulk resistance, R_B , in ohms
 α = a constant whose value generally lies between 10 and 40 volts⁻¹
 e = base of the natural logarithm = 2.718.

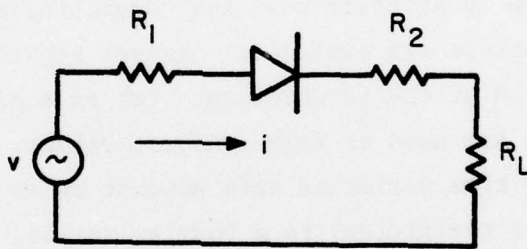


Figure 1. Diode mixer circuit.

The power series representation of Equation 1 is:

$$i = \sum_n k_n (v - V_b)^n, \quad n=0,1,2,\dots \quad (2)$$

where

$$k_n = \left. \frac{1}{n!} \frac{\partial^n i}{\partial v^n} \right|_{v=V_b}$$

V_b = the bias voltage.

In Figure 2, the magnitude of the power series coefficients relative to the second-order coefficient (in dB) are shown for a diode mixer (Reference 5). The abscissa value, i , is the current that flows for a given voltage, v .

Based on a fixed value of mixer forward bias voltage, a value of bias current is obtained using the graph in Figure 3. (Figure 3 was obtained using Equation 1.) The normalized power series coefficients are obtained using the graphs in Figure 2. The coefficients are then substituted into Equation 2 from which the nonlinear interactions are calculated.

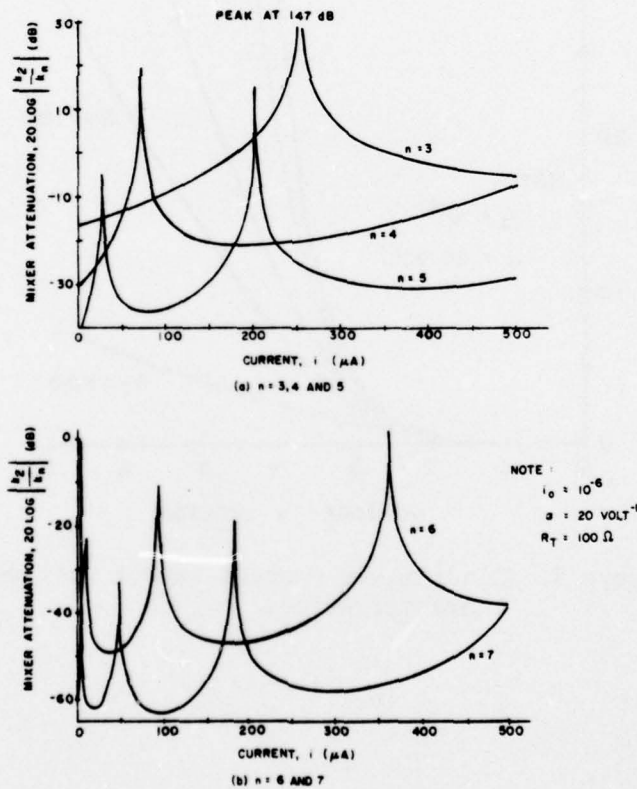


Figure 2. For diode mixer power series coefficients normalized to second-order coefficient, in dB.

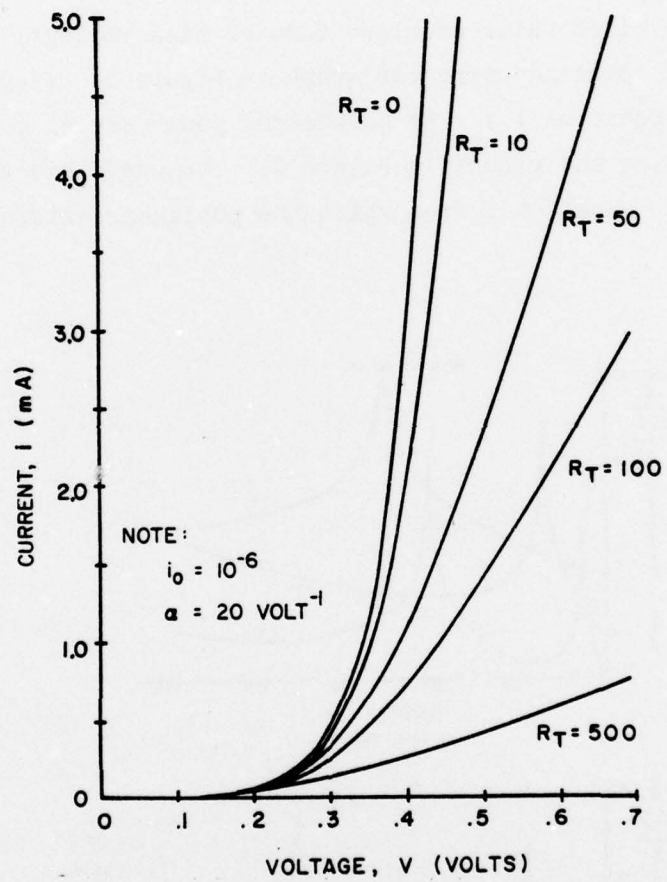


Figure 3. Diode mixer current versus voltage characteristics.

AN ILLUSTRATIVE EXAMPLE OF POWER SERIES LIMITATION

The following example illustrates the inapplicability of the power series for diode mixer analysis. Assume that the LO voltage is a sinusoid of peak amplitude equal to 0.63 volts. (This would correspond to an available power of 0 dBm for a 50-ohm signal generator. Virtually all mixers employ this level or greater to provide low conversion loss to the desired signal.) From Figure 3 it is seen that the current flowing at the positive peak of the LO waveform is approximately 2.5 mA (2,500 μ A), five times the maximum abscissa value on Figure 2. In fact, the abscissa value will vary from $-i_o$ to 2,500 μ A over each period of the LO waveform. In general, V_b (the true dc bias) is small compared to the peak-to-peak variation in the LO voltage. Thus, intuitively it is expected that one particular value of $20 \log k_2/k_n$ obtained from Figure 2 will not suffice. The coefficients will periodically take on all values shown on, and many more off, the scale of the figure. It is difficult to define a precise voltage limit for the usefulness of the power series. The number of terms needed for adequate convergence increases with increasing ac voltage levels and is dependent on the bias current. An optimistic limit is stated in the following inequality:

$$i_{LO} < \frac{1}{\alpha R_T} \quad (3)$$

where

$$i_{LO} = \text{the peak of the LO current waveform.}$$

In the previous example, $\alpha = 20 \text{ volts}^{-1}$, $R_T = 100 \text{ ohms}$, and $i_{LO} < 0.5 \text{ mA}$ will satisfy the inequality. The 0.5 mA corresponds to an LO power of

-14 dBm. An LO power of 0 dBm corresponds to 2.5 mA. For $\alpha = 40 \text{ volts}^{-1}$ and $R_T = 500 \text{ ohms}$, the LO power would be limited to -34 dBm by the preceding inequality. Thus, the power series is not useful for typical LO power levels.

It is shown in APPENDIX G that the power series for vacuum tubes will not converge in some practical situations.

SECTION 3

TAYLOR-FOURIER SERIES MIXER MODEL

BACKGROUND

A literature review of mixer analysis methods was conducted. A promising method was noted in References 2 and 3, but quantitative results were not presented.

The primary characteristic of the Taylor-Fourier method is the use of the Taylor-Fourier series. With this method, it is assumed that the LO level is much greater than the RF input levels. (See APPENDIX C for additional discussion of this point.) This method was tested as part of this task to see if it could be successfully applied to practical mixer analyses and could provide an accurate physical model of a mixer.

The Taylor-Fourier method was applied to two types of diode mixers: single-diode mixers (SDM) and double-balanced-diode mixers (DBDM). Computer models for predicting spurious responses based on circuit diagrams were prepared. For both types of mixers, the predictions were based only on the circuit passive component values, the LO voltages, a reference output voltage, and the diode characteristics. Mixer spurious-response measurements were made at ECAC and compared with predicted responses (Section 4). The procedures used to estimate the diode parameters on the basis of static or dc measurements are described in APPENDIX D.

THE TAYLOR-FOURIER METHOD

The procedures employed to model the SDM and DBDM apply in general to any mixer represented as a resistive, voltage-dependent, current source. The output current is related to the input RF voltage, v_{RF} , using:

$$i = \sum_{Q=0} \sum_{P=0} (v_{RF})^Q a_{P,Q} \cos (P2\pi f_{LO} t) \quad (4)$$

where

P, Q = integers representing the harmonic number of the LO and RF inputs, respectively, contributing to the response being analyzed

$a_{P,Q}$ = the Taylor-Fourier series response coefficients

f_{LO} = the local oscillator frequency

t = time.

USING THE RESPONSE COEFFICIENTS, $a_{P,Q}$

Once the response coefficients are known, the mixer output levels may be calculated from Equation 4 for any desired or undesired input voltage. However, Equation 4 can be put in a more convenient form for calculation purposes if the form of v_{RF} is given. For example, suppose v_{RF} consists of a single tone at a frequency that will cause a mixer response. Let:

$$v_{RF} = V_{RF} \cos 2\pi f_{RF} t \quad (5)$$

where

V_{RF} = peak voltage

f_{RF} = radio frequency.

A spurious response is said to occur when:

$$f_{RF} = \frac{P f_{LO} \pm f_{IF}}{Q} \quad (6)$$

where

f_{IF} = receiver intermediate frequency

f_{LO} = receiver local oscillator frequency.

Note, the desired response is among the set of responses described by Equation 6, but cannot be termed spurious. If the IF is the difference between the RF and LO frequency and if the LO is below the receiver's tuned frequency, then Equation 6 reduces to:

$$f_{RF} = f_{LO} + f_{IF}, \text{ receiver tuned frequency} \quad (7)$$

where

$$P = Q = 1.$$

In addition, the term of interest in Equation 4 that yields a component at f_{IF} when the input signal frequency satisfies Equation 7 is:

$$\begin{aligned} i_D &= (V_{RF} \cos 2\pi f_{RF} t) a_{1,1} \cos 2\pi f_{LO} t \\ &= a_{1,1} V_{RF}/2 \cos[2\pi(f_{RF} - f_{LO})t] + \dots \end{aligned} \quad (8)$$

where

i_D = the desired output of the mixer and additional outputs.

Thus, $a_{1,1}/2$ is the conversion transconductance of the mixer. (For this case, the $P=1, Q=3$ term of Equation 4 will also yield a component at f_{IF} . In fact, it is this term which describes the dynamic range of the mixer.)

The more general case, where f_{RF} is not restricted by Equation 7, may take on any value which satisfies Equation 6 for any integers P and Q , and either sign. For example, setting $P=2$ and $Q=3$ and sign = +, an input of frequency

$$f_{RF} = \frac{2f_{LO} + f_{IF}}{3} \quad (9)$$

will cause a response at the mixer output at the IF stage tuned frequency, f_{IF} . The amplitude of this response may be calculated by considering the appropriate, $P=2, Q=3$ term of Equation 4:

$$i_{SPUR} \doteq (V_{RF} \cos 2\pi f_{RF} t)^3 a_{2,3} \cos 4\pi f_{LO} t \quad (10a)$$

$$= \left(\frac{1}{2}\right)^3 V_{RF}^3 a_{2,3} \cos [2\pi(2f_{LO} - 3f_{RF})t] + \dots \quad (10b)$$

Using Equation 9:

$$i_{SPUR} \doteq \left(\frac{1}{2}\right)^3 V_{RF}^3 a_{2,3} \cos 2\pi f_{IF} t + \dots \quad (10c)$$

Thus $a_{2,3} V_{RF}^2/8$ is the conversion transconductance of the mixer for a $P=2, Q=3$ spurious response. A more general expression for Equation 10c is:

$$i_{\text{SPUR}} = \left(\frac{1}{2}\right)^Q V_{\text{RF}}^Q a_{\text{P,Q}} \cos 2\pi f_{\text{IF}} t \quad P > 0 \quad (11a)$$

and

$$i_{\text{SPUR}} = \left(\frac{1}{2}\right)^{Q-1} V_{\text{RF}}^Q a_{\text{P,Q}} \cos 2\pi f_{\text{IF}} t \quad P = 0 \quad (11b)$$

Equation 21 of APPENDIX C presents this relationship in terms of power output (referred to the input) versus power available at the input. Similar expressions may be employed to cover 2-signal intermodulation and other nonlinear effects.

CALCULATING THE RESPONSE COEFFICIENTS

In order to calculate the $a_{\text{P,Q}}$ values the following five steps were used and are suggested for use in developing additional models.

1. Model the current versus voltage characteristics of the nonlinear device. Figure 4 is an equivalent circuit diagram of the Ebers-Moll diode model (see Reference 6). The nonlinearity is represented by the relationship between v'_D and i_D using:

$$i_D = i_0 \left[e^{\alpha v'_D} - 1 \right] \quad (12)$$

where

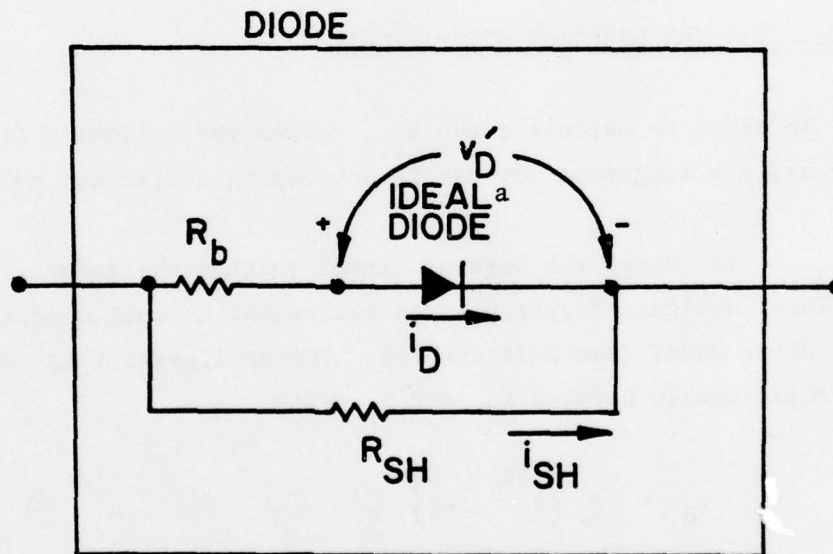
i_D = current through the ideal junction, in amperes

i_0 = reverse leakage current, in amperes

v'_D = voltage across the ideal diode junction, in volts

- α = diode parameter $\doteq q/kT$, volt⁻¹
 q = electric charge of an electron
 k = Boltzman's constant
 T = temperature in °K.

The value of the shunt resistance (R_{SH}) is generally very large, and therefore ignored in the mixer models. A computer program was prepared to calculate the values α and R_B that fit a set of measured dc characteristic data, as described in APPENDIX D.



^aAn ideal diode is governed by Equation 12.

Figure 4. Ebers-Moll diode model.

2. Write the loop or node equations for the circuit. For the SDM (Figure 5):

$$v_{RF} + v_{LO} = v_D' + i_D(R_S + R_b + R_L) \quad (13)$$

From Equation 12:

$$i_D = i_0 \left[e^{\alpha(v_{RF} + v_{LO} - i_D R_T)} - 1 \right] \quad (14)$$

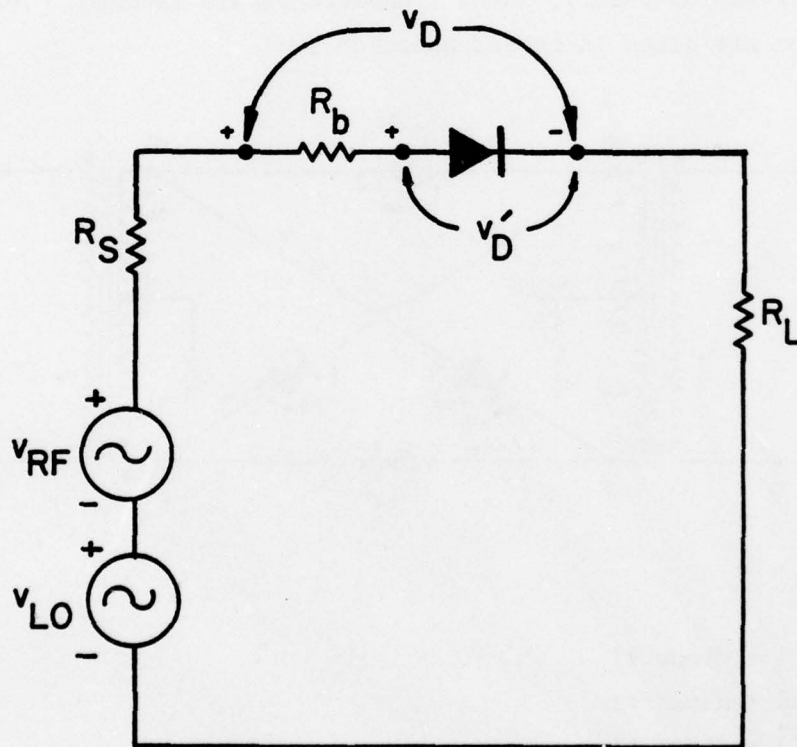


Figure 5. SDM circuit.

where

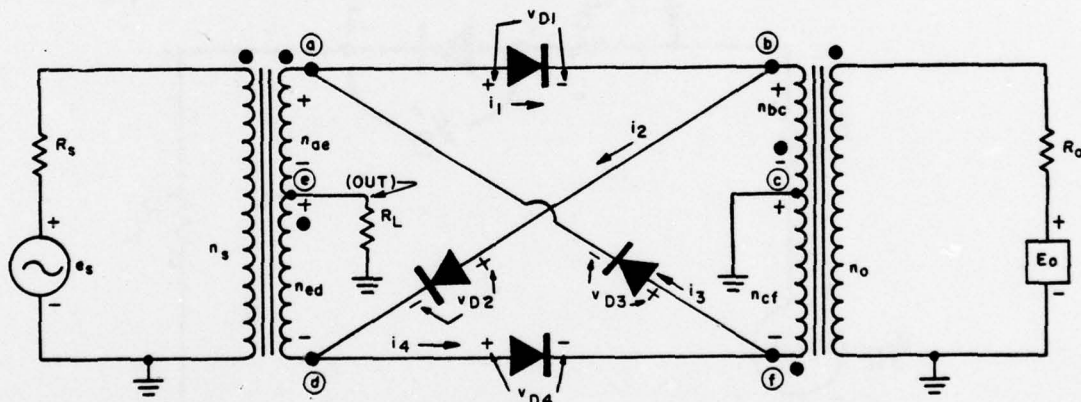
$$R_T = R_S + R_D + R_L = \text{total resistance}$$

$$R_S = \text{RF source resistance}$$

$$R_D = \text{bulk resistance}$$

$$R_L = \text{load resistance}$$

Step 2 was also accomplished for the DBDM. Figure 6 is the circuit diagram for the DBDM mixer. For this circuit, four loop equations are necessary; ideal transformers are assumed. These equations are given in matrix notation by:



NOTE:

D1 = diode #1

D2 = diode #2

D3 = diode #3

D4 = diode #4

Figure 6. Modeled DBDM circuit.

$$\begin{bmatrix} \frac{1}{\alpha_1} \ln \left(\frac{i_1}{i_{01}} + 1 \right) + k_3 E_0 - k_1 e_s \\ \frac{1}{\alpha_2} \ln \left(\frac{i_2}{i_{02}} + 1 \right) - k_3 E_0 - k_2 e_s \\ \frac{1}{\alpha_3} \ln \left(\frac{i_3}{i_{03}} + 1 \right) + k_4 E_0 + k_1 e_s \\ \frac{1}{\alpha_4} \ln \left(\frac{i_4}{i_{04}} + 1 \right) - k_4 E_0 + k_2 e_s \end{bmatrix} = \begin{bmatrix} A \end{bmatrix} \begin{bmatrix} i \end{bmatrix} \quad (15)$$

where

k_n = indicated turns ratio, secondary to primary-

E_0 = instantaneous LO voltage

e_s = instantaneous RF voltage

R_0 = LO source resistance

R_s = RF source resistance

i_{0j} = reverse leakage current for j^{th} diode

α_j = diode parameter for j^{th} diode

R_{bj} = bulk resistance for j^{th} diode.

$$\begin{bmatrix} k_1 = n_{ae}/n_s \\ k_2 = n_{ed}/n_s \\ k_3 = n_{bc}/n_0 \\ k_4 = n_{cf}/n_0 \end{bmatrix}$$

The members of $[i]$ are i_j where i_j is the forward current through j^{th} diode. The members of the $[A]$ are given by:

$$A_{1,1} = -k_1^2 R_s - k_3^2 R_0 - R_L - R_{b1}$$

$$A_{1,2} = -k_1 k_2 R_s + k_3^2 R_0 + R_L$$

$$\begin{aligned}
A_{1,3} &= +k_1^2 R_s - k_3 k_4 R_0 + R_L \\
A_{1,4} &= +k_1 k_2 R_s + k_3 k_4 R_0 - R_L \\
A_{2,2} &= -k_2^2 R_s - k_3^2 R_0 - R_L - R_{b2} \\
A_{2,3} &= +k_1 k_2 R_s + k_3 k_4 R_0 - R_L \\
A_{2,4} &= +k_2^2 R_s - k_3 k_4 R_0 + R_L \\
A_{3,3} &= -k_1^2 R_s - k_4^2 R_0 - R_L - R_{b3} \\
A_{3,4} &= -k_1 k_2 R_s + k_4^2 R_0 + R_L \\
A_{4,4} &= -k_2^2 R_s - k_4^2 R_0 - R_L - R_{b4} \\
A_{j,k} &= A_{k,j} \text{ for } j \neq k, j=1,2,3 \text{ and } 4
\end{aligned}$$

3. Derive expressions for the derivatives of the load resistor current with respect to the RF source voltage. This was done for as many as seven derivatives in both models. The derivatives for the SDM are contained in APPENDIX C; the first derivative for the DBDM is derived using:

$$\begin{bmatrix} -k_1 \alpha_1 J_1 \\ -k_2 \alpha_2 J_2 \\ +k_1 \alpha_3 J_3 \\ +k_2 \alpha_4 J_4 \end{bmatrix} = \begin{bmatrix} B \end{bmatrix} \begin{bmatrix} \frac{\partial i}{\partial e_s} \end{bmatrix} \quad (16)$$

where

$$\begin{aligned}
J_j &= (i_j + i_{0,j}) \\
B_{j,j} &= A_{j,j} \alpha_j J_j^{-1} \\
B_{j,k} &= A_{j,k} \alpha_j J_j \quad j \neq k
\end{aligned}$$

The expressions for the Q^{th} derivative have the general form:

$$[C^Q] = [B] \left[\frac{\partial^Q i}{\partial e_s^Q} \right] \quad (17)$$

The expressions for the $[C^Q]$ are in APPENDIX F.
The load resistor current is given using:

$$i_L = -i_1 + i_2 + i_3 - i_4 \quad (18)$$

Consequently:

$$\frac{\partial^Q i_L}{\partial e_s^Q} = -\frac{\partial^Q i_1}{\partial e_s^Q} + \frac{\partial^Q i_2}{\partial e_s^Q} + \frac{\partial^Q i_3}{\partial e_s^Q} - \frac{\partial^Q i_4}{\partial e_s^Q} \quad (19)$$

4. Derive expressions for the Taylor series coefficients using:

$$a_Q = \frac{1}{Q!} \frac{\partial^Q i_L}{\partial e_s^Q} \quad (20)$$

For the SDM, the a_Q values are given in APPENDIX C. Each a_Q value is dependent on the instantaneous value of the LO voltage; the a_Q values are periodic waveforms whose fundamental frequency is the LO frequency.

5. Calculate the $a_{P,Q}$ values using:

$$a_{P,Q} = \frac{1}{2\pi} \int_0^{2\pi} a_Q(t) d(\omega_{LO} t) \quad P=0 \quad (21)$$

$$a_{P,Q} = \frac{1}{\pi} \int_0^{2\pi} a_Q(t) \cos (P\omega_{LO} t) d(\omega_{LO} t) \quad P > 0 \quad (22)$$

where

$$\omega_{LO} = 2\pi f_{LO}$$

These coefficients are obtained by sampling the LO voltage time waveform. For each sample, the current and a_Q values are calculated; numerical integration is employed. To use Equation 22, the LO waveform must be an even function.

FREQUENCY-DEPENDENT RESPONSE COEFFICIENTS

In some cases, those frequency-dependent circuit parameters which cannot easily be isolated may become significant for analysis purposes. Some of these circuit parameters can be considered in the same manner as a bypass capacitor (a short circuit at high frequencies and an open circuit at lower frequencies). Where this is not possible, the Taylor series expansion in the Taylor-Fourier series method must be replaced by a Volterra series expansion. The additional complexities involved from this requirement will not be discussed here.

SECTION 4

RESULTS OF TAYLOR-FOURIER MODELING

Agreement is generally good between measured mixer spurious response levels and those predicted by the computerized Taylor-Fourier series models. The results were better for the SDM than for the DBDM apparently because of the sensitivity of certain responses of the DBDM to the dc diode and other circuit parameters (especially their degree of balance). Other DBDM responses (described in this section) are generally insensitive.

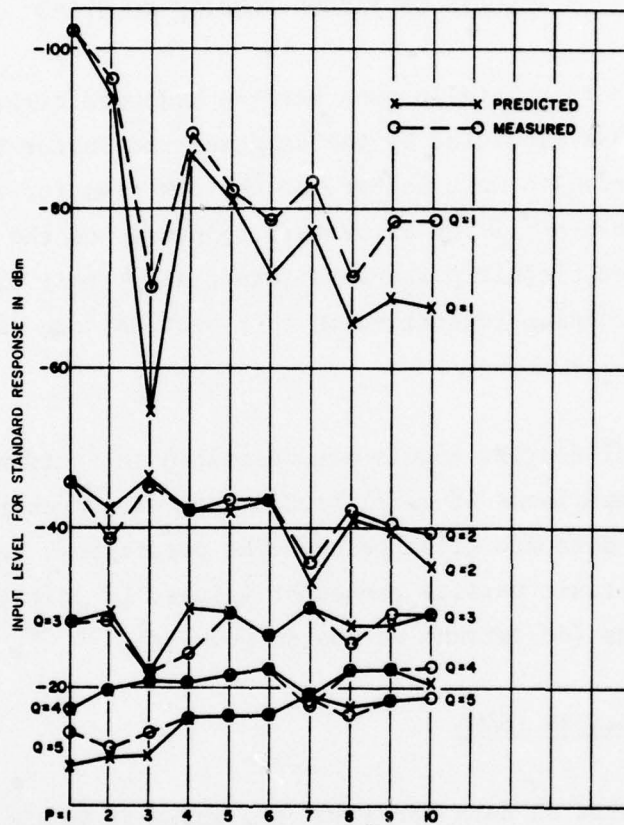
The Taylor-Fourier models are described in Section 3 and APPENDIX C. Results of comparisons of model predictions with measured spurious response (SR) data are given below. The predictions were based only on the nominal circuit passive component values, LO voltages, and dc diode characteristics (dc current versus dc voltage).

SINGLE-DIODE MIXERS (SDM)

The measured SR data for a SDM are shown in TABLE 1(a) of APPENDIX C;⁷ the corresponding predictions are shown in TABLE 1(b). Forty-two of the predicted values (over half) differ by less than 1 dB from the measured values. The average difference is 1 dB and the standard deviation of the differences is 3.1 dB. Some of the data are shown on Figure 7.

A significant conclusion from a parameter sensitivity study was that good prediction accuracies are obtainable with uncertainties of up to 25% in the diode parameter α and a factor of 10 in the leakage

⁷ECAC lab memo #7769 May 1977.



Q = harmonic number of input signal frequency

P = harmonic number of LO frequency

(see Equation C-2 of APPENDIX C)

Figure 7. Measured and predicted spurious response values for SDM.

current. This information is of value to a desk-bound analyst. The sensitivity analysis results are presented in TABLES 2(a) and 2(b) of APPENDIX C. Note that the standard error is minimum when the values of i_0 and α , determined by examining the dc diode characteristic, are employed. Similar results were obtained when the LO voltage was increased from 0.47 to 1.66 volts, as shown in TABLES 4(a) and 4(b) of APPENDIX C.

DOUBLE-BALANCED-DIODE MIXERS (DBDM)

Measured SR data for Hewlett-Packard HP10534a and HP10514a mixers were obtained at ECAC⁸ as noted in TABLES 1 and 2. The HP10534a was found to have a defective diode prior to testing. Its diodes were replaced by four new 1N82 diodes after the dc characteristics of these diodes were measured. The circuit diagram for the HP10534a is given in Figure 6; a large number of DBDM's use this circuit.

DBDM Predicted Responses

The predicted responses for the HP10534a circuit are given in TABLE 3. For several responses, the predictions varied greatly from the measured data. A parameter sensitivity study indicated that these responses were among several that were sensitive to the diode parameters and/or to the balance among the diodes.

DBDM Parameter Sensitivity Study

The DBDM model was employed to perform a study in which the diode parameters -- α , i_0 , and R_b -- were varied about the center values selected by the procedure of APPENDIX D. The variations were as follows:

⁸ECAC lab memo #77-73.

TABLE 1
 MEASURED SPURIOUS RESPONSE LEVELS FOR HEWLITT-
 PACKARD HP10534a DOUBLE-BALANCED MIXER ^{a, b}

$\pm Q$ P	+1	-1	+2	-2	+3	-3	+4	-4	+5	-5	+6	-6	+7	-7
1	-117	-117	-44	-42	-37	-38	-23	-24	-26	-26	-18	-19	-21	-20
2	-102	-101	-19	-38	-35	-34	-23	-25	-23	-23	-21	-19	-20	-22
3	-109	-112	-44	-43	-35	-35	-27	-25	-25	-25	-18	-21	-21	-19
4	-85	-92	-40	-41	-36	-35	-22	-26	-24	-26	-17	-19	-18	-18
5	-106	-106	-38	-29	-39	-40	-25	-23	-22	-23	-20	-18	-21	-20
6	-89	-93	-44	-41	-34	-33	-26	-25	-21	-22	-19	-18	-20	-21
7	-97	-96	-45	-45	-35	-35	-25	-26	-25	-24	-16	-13	-18	-16
8	-91	-81	-38	-41	-40	-58	-23	-22	-27	-27	-21	-21	-17	-16
9	-93	-86	-46	-45	-35	-37	-24	-22	-25	-27	-15	-17	-18	-18
10	-80	-85	-40	-41	-37	-38	-27	-26	-22	-20	-21	-21	-22	-21

^a Values are the input levels, in dBm, required to produce a standard response level at the output of -123 dBm.

^b P_{LO} = 0 dBm.

TABLE 2
 MEASURED SPURIOUS RESPONSE LEVELS FOR HEWLETT-
 PACKARD HP10514a DOUBLE-BALANCED MIXER ^{a, b}

P	+0	+1	-1	+2	-2	+3	-3	+4	-4	+5	-5	+6	-6	+7	-7
1	-111	-111	-111	-30	-35	-34	-38	-22	-22	-26	-27	-19	-17	-20	-20
2	-74	-76	-76	-30	-29	-30	-25	-14	-15	-21	-21	-9	-13	-21	-18
3	-102	-103	-103	-34	-34	-35	-33	-22	-15	-18	-19	-12	-12	-15	-17
4	-71	-79	-79	-23	-24	-32	-33	-19	-18	-23	-25	-10	-9	-14	-14
5	-101	-100	-100	-26	-24	-37	-34	-24	-25	-26	-25	-19	-20	-16	-15
6	-71	-72	-72	-27	-26	-22	-25	-15	-16	-25	-24	-13	-13	-21	-21
7	-92	-86	-86	-30	-39	-33	-33	-22	-21	-23	-23	-18	-18	-20	-21
8	-65	-67	-67	-26	-26	-28	-26	-14	-14	-21	-22	-13	-12	-19	-19
9	-83	-79	-79	-31	-30	-38	-38	-16	-17	-22	-22	-16	-16	-21	-21
10	-67	-65	-65	-23	-22	-30	-30	-14	-13	-20	-19	-12	-13	-18	-17

^aValues are the input levels, in dBm, required to produce a standard response level at the output of -119 dBm.

^bP_{LO} = +1 dBm.

For α : $\alpha + 5$

For j_0 : $2i_0$ and $j_0/2$

For R_b : $2R_b$ and $R_b/2$.

Most responses remained relatively unchanged for the input values. A few responses were significantly weaker for a given set of diode parameters. These were among the responses that disappear for a perfectly balanced DBDM. The results also indicated that the best overall predictions were obtained by increasing the α value of diode #2 (D2, Figure 6).

This change made diode #2 more nearly equal to the other diodes in parameter values. It was noted that the measured dc data for this diode resulted in the worst "fit" in terms of rms deviation to the Ebers-Moll diode model. The predicted SR values, with the increase of α_2 by 5 volts⁻¹, are given in TABLE 4. Apparently, the representation of this diode was lacking.

A Perfectly Balanced DBDM

Three-fourths of the responses (i.e. if either P or Q is even) completely disappear under the unlikely situation of four *identical* diodes and where other circuit parameters are balanced regardless of the actual parameter values. The model predictions for a set of four identical diodes is shown in TABLE 5. The sets of measurements in TABLES 1 and 2 do not approach this ideal mixer response behavior.

Another characteristic of the perfectly balanced response calculations is that the remaining (where both P and Q are odd, TABLE 5) responses are similar in level to their values for the slightly unbalanced data (e.g., TABLE 3). Apparently, these responses are not strongly dependent on the degree of balance.

TABLE 3
 PREDICTED SPURIOUS RESPONSE LEVELS FOR HEWLETT PACKARD HP10534a DBDM

Q + P +	1	2	3	4	5	6	7
1	-117.3	- 30.6	- 23.6	- 19.9	- 22.1	- 19.1	- 19.1
2	- 76.9	- 43.8	- 24.9	- 26.1	- 22.8	- 22.5	- 20.9
3	-101.2	- 39.9	- 28.6	- 22.2	- 24.7	- 19.4	- 21.0
4	- 68.3	- 43.1	- 20.1	- 26.2	- 23.1	- 22.5	- 20.9
5	- 58.4	- 42.2	- 31.5	- 23.9	- 25.5	- 20.5	- 21.6
6	- 60.0	- 40.5	- 25.2	- 26.1	- 23.3	- 22.4	- 20.9
7	- 89.8	- 42.8	- 32.8	- 24.9	- 25.9	- 21.1	- 21.9
8	- 69.9	- 13.9	- 27.6	- 25.8	- 23.5	- 22.3	- 20.8
9	- 89.1	- 42.3	- 33.1	- 25.5	- 26.1	- 21.4	- 22.0
10	- 71.4	- 39.7	- 28.5	- 25.1	- 23.5	- 22.1	- 20.7

TABLE 4
 PREDICTED SPURIOUS RESPONSE LEVELS FOR HEWLETT PACKARD
 HP10534a DBDM, WITH α_2 INCREASED BY 5 VOLTS⁻¹

Q + P +	1	2	3	4	5	6	7
1	-117.3	- 26.7	- 21.3	- 20.7	- 22.5	- 19.3	- 19.4
2	- 82.9	- 41.0	- 23.9	- 25.0	- 24.2	- 21.8	- 21.4
3	-101.9	- 36.2	- 29.0	- 20.5	- 24.9	- 18.2	- 21.1
4	- 63.3	- 40.2	- 25.7	- 25.0	- 24.2	- 21.8	- 21.4
5	- 79.0	- 37.9	- 31.7	- 22.3	- 25.7	- 19.6	- 21.7
6	- 75.6	- 38.1	- 27.7	- 24.9	- 24.2	- 21.8	- 21.3
7	- 88.6	- 38.5	- 32.9	- 23.2	- 26.1	- 20.2	- 22.0
8	- 78.7	- 31.4	- 26.9	- 24.7	- 24.2	- 21.7	- 21.2
9	- 89.0	- 38.2	- 33.3	- 23.8	- 26.3	- 20.6	- 22.2
10	- 77.9	- 35.2	- 29.3	- 24.2	- 24.0	- 21.6	- 20.9

TABLE 5
 HYPOTHETICAL PERFECTLY BALANCED DBDM RESPONSES

Q → P ↓	1	2	3	4	5	6	7
1	-117.3		- 22.3		- 23.0		- 19.6
2					- 13.0 ^a		- 12.5 ^a
3	-101.4		- 29.4		- 24.9		- 20.9
4					- 11.7 ^a		- 11.6 ^a
5	- 66.7		- 31.9		- 25.6		- 21.5
6					- 12.7 ^a		- 12.5 ^a
7	- 90.0		- 33.1		- 26.0		- 21.7
8					- 12.3 ^a		- 12.0 ^a
9	- 89.6		- 33.4		- 26.1		- 21.8
10					- 12.3 ^a		- 12.1 ^a

NOTE: Blank spaces indicate that calculated power levels were nearly equal to or greater than the LO power level.

^a These values can be shown to be nonexistent (blank, as above) for a perfectly balanced mixer. They represent quantizing computer noise.

SECTION 5

POWER SERIES COMPARED WITH TAYLOR-FOURIER SERIES

The most significant differences between the power series and Taylor-Fourier series with regard to modeling a receiver mixer are as follows:

1. Using the power series, the mixer nonlinearity is represented by the LO amplitude and a series of coefficients, the minimum number of which is equal to the highest sum of the harmonic numbers of the LO and RF signals involved in the mix (i.e., P and Q, respectively).

2. Using the Taylor-Fourier series, representation of the mixer nonlinearity requires a matrix of coefficients; one coefficient for every combination of P and Q involved.

Use of the power series for the prediction of spurious response or intermodulation provides results which differ substantially from measured results. An examination of two of these erroneous results follow.

1. For a fixed input level, V_{RF} , the output level for a $P=i$, $Q=j$ spurious response is calculated by multiplying the $P=j$, $Q=i$ output level by the factor

$$(V_{LO}/V_{RF})^{i-j}$$

which produces results contrary to measured results.

2. For an increase in the LO voltage by a factor, a given spurious response output level will increase by that factor raised to

the p^{th} power; e.g., an increase of the LO by 10 dB will increase a $P=5$ response by 50 dB. In practice, however, a decrease usually occurs.

Thus, a receiver mixer model based on the power series will generally lead to confusing and inaccurate predictions while the Taylor-Fourier series models are consistent with experienced results.

SECTION 6

CONCLUSIONS

1. The use of power series time-constant coefficients to predict or model mixer spurious or RIM responses should be avoided.

2. The use of Taylor-Fourier series coefficients to predict and model mixer spurious or RIM responses can provide reasonably accurate results. Models are described for two types of mixers and instructions are included for developing additional models.

3. Reasonable estimates of high-order RIM responses can be made on the basis of measured values of low-order RIM responses. This estimation problem is more difficult for situations involving double-balanced-diode mixers because many of the RIM responses depend on the degree to which the mixer is balanced. A rule-of-thumb factor for dealing with this situation is provided in APPENDIX A.

APPENDIX A

COSAM REQUIREMENTS FOR INCLUSION OF ADDITIONAL
INTERMODULATION (IM) PRODUCTSBACKGROUND

One type of IM problem exists for which measured data will rarely be available, because this type is not considered in MIL-STD-449 measurement procedures. Many cases of measured IM that are not predicted in a recent evaluation of COSAM performance in the high frequency (HF) band⁹ could be explained by products of the type noted in Equation A-1. COSAM is a computer model for the prediction of communications systems performance in a cosite configuration.

The Frequency Relationships

Recent measurements at ECAC that involved an HF receiver have revealed a type of IM response; this response has been ignored in the past and is a subset of the following equation:

$$\pm mf_1 \pm nf_2 \pm pf_{LO} = f_{IF} \quad (A-1)$$

where

m, n, p = positive integers

f₁, f₂ = input signal frequencies

f_{LO} = the receiver first local oscillator
frequency

f_{IF} = the receiver first IF.

⁹M. Lustgarten, et al, *Performance of the Cosite Analysis Model (COSAM) for Selected HF Equipments*, ESD-TR-76-010, ECAC, Annapolis, MD, November 1976.

Equation A-1 represents a set of equations.

The usual IM interaction involves the following subset of Equation A-1:

$$\begin{aligned} \pm mf_1 \pm nf_2 &= f_0 && (A-2) \\ (\text{i.e., for } p &= \pm 1) \end{aligned}$$

where

$$f_0 = \text{the receiver tuned frequency} = f_{LO} \pm f_{IF}$$

Note that if $n=0$, Equation A-1 describes a set of common spurious responses.

Another type of interaction noted in the HF measurements was:

$$\begin{aligned} \pm mf_1 \pm nf_2 &= f_{IF} && (A-3) \\ (\text{i.e., for } p &= 0) \end{aligned}$$

Measurements made using MIL-STD-449 procedures *only* consider interactions that involve Equation A-2 and, more recently, a subset of Equation A-3 (i.e., the subset where $m = n = 1$).

The remaining subsets of Equation A-1 (i.e., for $p = \pm 1$ and $p \geq 2$) were also noted in the HF measurements. The IM interactions normally considered are subsets of Equation A-1 such that $p = \pm 1$ (the sign is determined by receiver design) and $m + n = 2, 3, 5$ and 7 . Recent measurements¹⁰ indicate that these subsets do not take into account approximately 80% of the potential (2-signal) IM cases. Most of these additional IM cases were for $p = 0, \pm 1$ and $p = 2$ and 3 . A few were for $p = \pm 1$ and

¹⁰ECAC lab memo: "KWM-2 IM Tests in Support of Model Development," April 1976.

$m + n = 4$ and 6 . Some study and additional measurements are needed to determine the most significant cases.

Power Transfer Relationships

Given that the frequency relationships exist for the usual 2-signal IM interaction, the level of RIM interference can be computed using:

$$P_{ino} = m (P_a - \beta_a) + n (P_b - \beta_b) - K_{m,n} \text{ (or } K'_{m,n}) \text{ dBm} \quad (\text{A-4})$$

where

P_{ino} = the equivalent on-tune input interference power that results in the same output interference as the combined IM effect of P_a and P_b

P_a = the receiver input level due to source a

P_b = the receiver input level due to source b

β_a = the receiver rejection prior to the nonlinearity at frequency of source a

β_b = the receiver rejection prior to the nonlinearity at frequency of source b

$K_{m,n}$ = the normalized nonlinear conversion coefficient for order $m + n$ of the mixer

$K'_{m,n}$ = the normalized nonlinear conversion coefficient for the RF amplifier.

Because the usual IM involves only the $p = +1$ case, only two subscripts of K and K' were needed. Methods were required to calculate K values for the additional types of IM that involve interactions occurring primarily in the mixer circuits of receivers. Measured data will rarely be available.

The NCAP Computer Program

The Nonlinear Circuit Analysis Program (NCAP), a computer program obtained from RADC, permits the analyst to estimate a class of nonlinear effects in receivers that involve small signals. However, mixers are generally operated as "large signal" nonlinear devices; i.e., local oscillator levels that are necessary for efficient mixer operation are large enough such that basic assumptions in the NCAP models do not generally apply.

EXTRAPOLATION OF $K_{m,n}$ VALUES

Predictable trends in response levels exist for most mixer types and should greatly ease the implementation of additional IM products for COSAM. These are evident by the Taylor-Fourier series models and are supported by measured data.

The COSAM parameters, $K_{m,n}$, are directly related to Taylor-Fourier coefficients, $a_{1,Q}$ for $Q = m + n$. In general, however, the values for $a_{p,Q}$ are necessary to predict the additional IM products.

The antilogs of COSAM parameters, $K_{m,n}$, are inversely proportional¹¹ to the Taylor-Fourier series coefficients, $a_{1,m+n}$. As mentioned earlier, the only subset of Equation A-1 presently considered by COSAM is the $P=1$ subset (note $Q = m + n$). Therefore, $K_{m,n}$ may be considered a measure of $a_{1,m+n}$. The objective is to find the relationship between $a_{1,m+n}$ and the more general $a_{p,m+n}$. For a given $m + n$, the $a_{p,m+n}$ are the Fourier series coefficients of the periodic time functions $a_{m+n}(t)$.

¹¹Maiuzzo, M., "Models of Nonlinear Receiver Interactions," 1975 IEEE EMC Symposium Record, San Antonio, TX, October 1975.

To extend the COSAM capability, $K_{m,n}$ values for other than the $P=1$ case are needed. For purposes of discussion, the notation $K_{m,n,(P)}$ will be employed where the usual $K_{m,n} \stackrel{\text{def}}{=} K_{m,n(1)}$ from the proportion (see Reference 11):

$$K_{m,n(P)} = K_{m,n(1)} + 20 \log (a_{1,m+n}/a_{P, m+n}) \quad (\text{A-5})$$

For the cases of most interest, i.e. where $m + n \geq 2$, the second term is usually less than a few dB.

Some exceptions may be noted in the case of balanced mixers. For $m + n$ odd (the usual IM case considered by COSAM) and P odd, the second term of Equation A-5 can be shown to have approximately a value of $-20 \log P$. For $m + n$ odd and P even, the value of the second term of Equation A-5 is dependent on the degree of balance of the mixer (-20 dB seems typical). The other case considered by COSAM is $m + n = 2$, where the second term of Equation A-5 does not seem to have a simple relationship with the value of P .

BASIS FOR EXTRAPOLATION

The $a_{p,Q}$ are the Fourier series coefficients of the periodic Taylor series coefficients $a_Q(t)$. Given the general shape of an $a_Q(t)$, reasonable estimates of its frequency spectrum or Fourier series can be made.

Most mixers behave as switches, either on-off or plus-minus in the case of balanced mixers. Thus the instantaneous transconductance, $a_1(t)$, can be approximated by a trapezoidal-like waveform. The IM products of interest, however, involve the $Q \geq 2$ coefficients; e.g., $a_2(t)$ is one-half the rate of change of a_1 with respect to the RF driving voltage, as a function of time. This coefficient has its maximum value when the mixer is

turning on or off (a much shorter period of time than the width of $a_1[t]$). Thus, the spectrum of $a_2(t)$ approaches the spectrum of an impulse, and stays fairly constant with P^a . The higher-Q-order $a_Q(t)$ coefficients are more "impulse-like." Note that they only appear as impulses over the range of P values of interest. Given the actual pulse widths of the $a_Q(t)$, bandwidths may be calculated. In the case of a perfectly balanced mixer, the even-order $a_Q(t)$ coefficients are always zero; as a result the $a_{p,Q}$ values are also zero for even values of Q. However, 20 dB additional rejection seems to be typically realized. Also, for perfectly balanced mixers, with Q odd and P even, the $a_{p,Q}$ coefficients are non-existent because of odd symmetry of $a_Q(t)$ about the time where the LO changes sign. For these coefficients, 20 dB more rejection than the (P-1, Q) response is typically achieved

COEFFICIENTS INVOLVING Q=1

As mentioned above, the $a_1(t)$ waveform is almost trapezoidal. Thus, the coefficient values $a_{p,1}$ have an amplitude envelope which can be calculated using:

$$\begin{aligned} M_p &= 1/P, & \Pi P f_{LO} t_r < 1 \\ M_p &= 1/P^2, & \Pi P f_{LO} t_r > 1 \end{aligned} \quad (A-6)$$

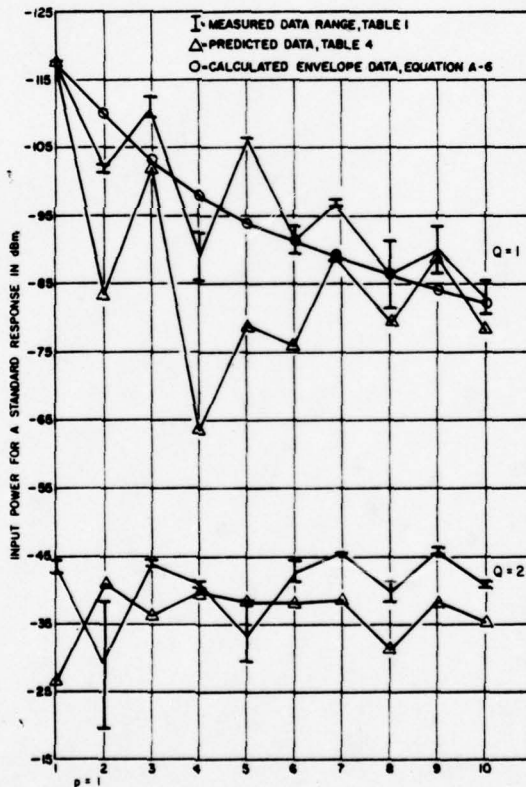
where

M_p = calculated envelope of $a_{p,1}$ coefficients. The input power for a standard response for a (P,1) response will be $-20 \log M_p$, in dB, relative to the (1,1) input power

t_r = rise time of the $a_1(t)$ waveform, approximated by a trapezoidal waveform.

^aThese near-impulses are nearly 90° out of phase with the LO; therefore, the coefficients will increase in value with, and in some cases may even be proportional to P.

This envelope is plotted in Figure A-1 for one of the measured DBDM's. The rise time was taken from the computer program output. Note that the peaks of both the measured and the predicted values are, with one exception, near the envelope. However, several predicted values lie in nulls that are deeper than those for the measured responses. The cause for these optimistic DBDM predictions is not precisely known. The discrepancies are the result of an imbalance in the circuits. It is more realistic to employ, for $a_{p,1}$ predictions involving DBDM's, the envelope of the $Q=1$ data and an additional 10 or 20 dB rejection for even order P values.



Q = harmonic number of input signal frequency
 P = harmonic number of LO frequency
 (see Equation C-2 of APPENDIX C)

Figure A-1. Measured and predicted spurious response values for DBDM.

APPENDIX B

APPLYING MIXER SR REJECTION VALUES TO
RECEIVER REJECTION CALCULATIONSBACKGROUND

When estimating receiver rejection to a spurious response the mixer SR rejection values should not be used directly, and the rejection (dB) of the receiver front-end added to the mixer rejection is not sufficient in most cases. The latter method has been used in the past.

The mixer rejection to a given (P,Q) spurious response $R_{P,Q}$ is the difference between the input levels (in dBm) for the (1,1) response and for the (P,Q) response. A standard output response level is fixed in both cases; usually this output level is slightly greater (say 10 dB) than the noise level at the output. However, because of the nonlinearity involved, the amount of rejection is highly dependent on the standard response level chosen for the test. Moreover, in a receiver the noise levels at the mixer output are likely to be quite different from those present during the breadboard test of an isolated mixer circuit. Fortunately, a simple correction is possible if the amount (E) is known by which the output standard response level differs from breadboard to working receiver.

A SIMPLE CORRECTION

The receiver's rejection can be calculated using:

$$\beta_{SR} = R_{P,Q} + \beta_{FE} - (Q-1) E/Q \quad (B-1)$$

where

β_{SR} = the receiver's rejection to the spurious response in question, in dB. That is, the difference between the receiver input level required to cause a receiver standard response of (usually) 10 dB (S+N)/N, first at the receiver's tuned frequency and, second, at the spurious response frequency.

$R_{P,Q}$ = the mixer's rejection to that SR, in dB

$$E = E_R - E_M$$

E_R = the level at the mixer output (if the receiver input is on-tune) that results in a receiver standard response (i.e., the receiver input is at the receiver sensitivity level), in dBm

E_M = the mixer output reference level used during the SR rejection measurements of the mixer alone, in dBm

β_{FE} = the rejection relative to on-tune provided by the receiver's front end stages to a signal at the SR frequency, in dB.

AN EXAMPLE

In TABLE 2 the rejection to a (2,2-) SR is 82 dB for a HP model 10514 double-balanced diode mixer (DBDM). Here $R_{P,Q} = 82$ dB. The output reference level is $-111 - 8 = -119$ dBm; the conversion loss for the (1,1+) response was measured at 8 dB. Thus, $E_M = -119$ dBm. Now, if this mixer is used in a receiver where the front-end gain is 24 dB and whose sensitivity is -105 dBm, the mixer output level E_R will be $-105 + 24 - 8 = -89$ dBm. The parameter E in Equation B-1 then, $E = -89 -$

(-119) = 30 dB. (Note also that the conversion loss of 8 dB is cancelled in the computation of E and its value is arbitrary for these calculations.) Thus, from Equation B-1, the receiver's rejection to the (2,2,-) response is:

$$\beta_{SR} = 82 + \beta_{FE} - (2-1) (30)/2$$

or

$$\beta_{SR} = 67 + \beta_{FE}, \text{ in dB} \tag{B-2}$$

This example is presented graphically in Figure B-1.

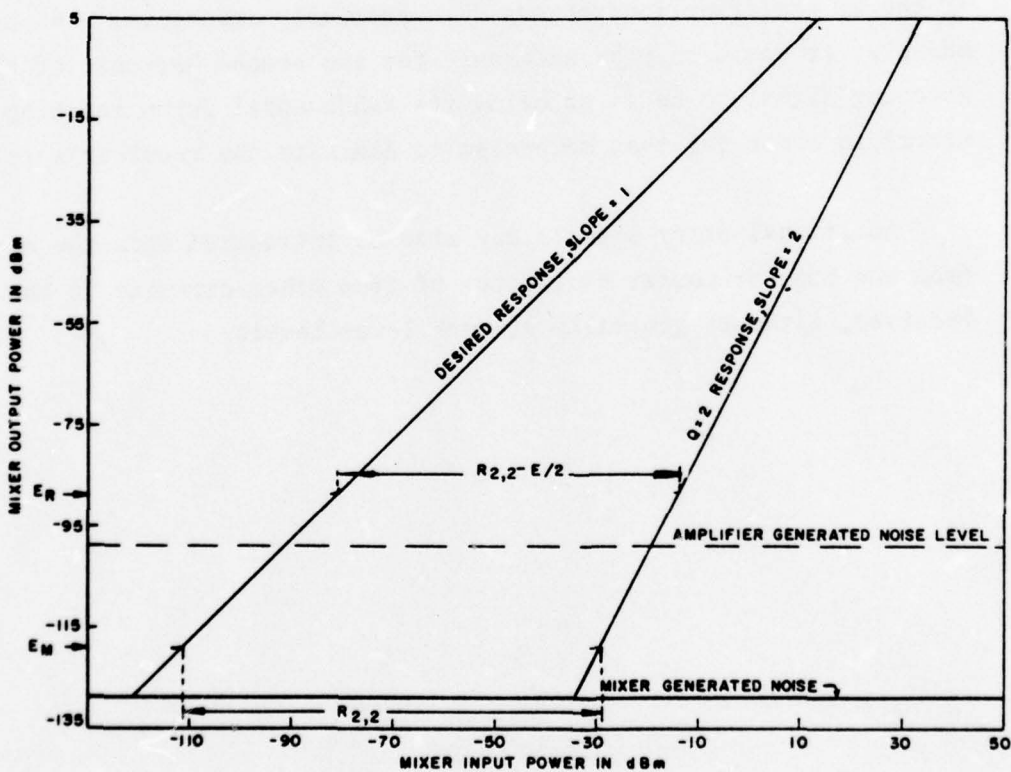


Figure B-1. Graphical presentation of example problem.

AN ADDITIONAL CONSIDERATION

Harmonic levels generated by the radio frequency (RF) amplifiers can be an important factor in a receiver's rejection to a spurious response (SR), or IM response for that matter. For example, refer to TABLE 2. The rejection to the P=2, Q=1 (+) response is 44 dB less than the rejection to the P=2, Q=2 (+) response. Because of its frequency, the second harmonic of the signal entering the receiver at the (2,2,+) SR frequency will pass through the mixer with the rejection accorded to a (2,1,+) response. It would not be difficult to construct an example whereby this mechanism would determine the receiver's rejection to a SR. It would be important to include this mechanism if the SR frequency fell below the tuned frequency and/or if the RF amplifier interstages were extremely selective. In our example, it would only be necessary for the second harmonic of the incoming signal to be 44 dB below its fundamental (upon reaching the mixer) in order for that mechanism to dominate the receiver's response.

Additional stray signals may also be introduced into the mixer from the base or master oscillator or from other circuits in the receiver, although generally at much lower levels.

APPENDIX C

"A COMPUTER PROGRAM FOR THE PREDICTION OF DIODE MIXER SPURIOUS
RESPONSE LEVELS FOR CONDITIONS INCLUDING LARGE LOCAL OSCILLATOR LEVELS"^a

Mike Maiuzzo

^aReprint as seen in *IEEE International Symposium on Electromagnetic
Compatibility*, Seattle, WA, 2-4 August 1977.

A COMPUTER PROGRAM FOR THE PREDICTION OF DIODE MIXER SPURIOUS
RESPONSE LEVELS FOR CONDITIONS INCLUDING LARGE LOCAL OSCILLATOR LEVELS

M. A. Maiuzzo
IIT Research Institute
ECAC, North Severn
Annapolis, MD 21402

Summary

The conversion transconductance of mixers increases with increasing local oscillator drive level. The rejection of unwanted nonlinear outputs such as intermodulation and spurious responses also generally improves with local oscillator level. Small-signal analysis techniques, including conventional employment of the Taylor series and Volterra series, are not applicable under these conditions and can lead to large errors in the estimation of rejection values.

A procedure for the calculation of wanted and unwanted response levels is presented. The procedure employs techniques applicable to conditions of either large or small local oscillator drive levels. Accurate predictions are shown to be obtainable based on knowledge of linear circuit parameters, direct-current diode characteristics and applied voltages. Comparisons of predictions with measured nonlinear response levels are made and the method is shown to be accurate.

The model also indicates that, for practical mixers, the responses are not overly sensitive to the diode parameters. Good prediction accuracies are obtained with uncertainties of up to 25% in the diode parameter α and a factor of ten in the reverse leakage current.

Introduction

Numerous investigators have developed models of diode mixer nonlinear responses. However, reported procedures have in general been unsatisfactory for practical predictions of spurious responses, based solely on diode DC characteristics. In realistic situations, the local oscillator (LO) level is large. The analyses of references 1 and 2, for example, rely on the small-signal assumption.

One technique which has found success in large-signal intermodulation analyses is the Fourier-Bessel series expansion.³ It has recently been applied to the analysis of intermodulation in Classes B and C transmitter amplifiers.^{4,5}

In this paper, a Taylor-Fourier series expansion is applied to the prediction of diode mixer spurious responses. The equation for the static diode transfer is given by¹:

$$i = i_0 \left[e^{\alpha(v - iR_b)} - 1 \right] \quad (1)$$

where

i = diode current
 i_0 = reverse leakage current
 v = diode voltage
 R_b = diode bulk resistance

The model is based on the following concept. Each power series coefficient of the expansion of the diode current is treated as a periodic time variable. The amplitude and period of each is determined by the amplitude and period of the LO drive. Each coefficient is then expanded in a Fourier series. The integration

process which provides the Fourier coefficients also provides the smoothing of the predictions with respect to the input data.

Terman⁶ has described the technique in a discussion of spurious responses. His example consists of the Fourier expansion of the transconductance, the first term of the power series. RADC/SIGNATRON⁷ discuss the technique in more detail. A spurious response is said to occur when an input signal is at a frequency, f_{sp} , such that equation (2) is satisfied.

$$f_{SP} = \frac{P f_{LO} \pm f_{IF}}{Q} \quad (2)$$

where

f_{LO} = LO frequency
 f_{IF} = the IF, or desired output frequency
 P = the harmonic number of the LO frequency contributing to the response at f_{IF}
 Q = the harmonic number of the input signal frequency, f_{sp} , contributing to the response at f_{IF} .

It is shown that the method of analysis reported in this paper does allow accurate prediction of mixer spurious responses.

Summary of the Approach

The static DC output current vs. applied source voltage characteristics is expanded in a truncated Taylor series:

$$i = \sum_{Q=0}^7 a_Q (v_t - B)^Q \quad (3)$$

where

v_t = total Thevenin equivalent applied voltage

$$a_Q = \frac{i}{Q!} \frac{\partial^Q i}{\partial v^Q} \quad (4)$$

and a_Q is evaluated for v_t equal to the "bias", or operating point voltage. For this case the circuit's DC transfer characteristic is given by:

$$i = i_0 \left[e^{\alpha(v_t - iR_T)} - 1 \right] \quad (5)$$

where

$R_T = R_S + R_b + R_L$ (6)
 R_S = Thevenin equivalent source resistance
 R_L = load resistance

$$\frac{\partial i}{\partial v_t} = I_0 \left[\alpha - \alpha R_T \frac{\partial i}{\partial v_t} \right] e^{\alpha(v_t - iR_T)} \quad (7)$$

Noting:

$$e^{\alpha(v_t - iR_T)} = \frac{i}{I_0} + I \quad (5a)$$

Then:

$$\frac{\partial i}{\partial v_t} = \frac{\alpha(i + I_0)}{1 + \alpha R_T(i + I_0)} \quad (8)$$

From (4):

$$a_1 = \frac{\alpha(I + I_0)}{1 + \alpha R_T(I + I_0)} \quad (9)$$

where I is the value of i which satisfies equation (5) with the bias voltage substitute for v_t . The numerical solution of (5) employs both Newton-Raphson and successive substitution methods. The expressions for a_2 through a_7 are presented in APPENDIX I.

Up to this point, the analysis has been the same as a standard small signal analysis. The departure comes from treating the local oscillator drive voltage as a time-varying bias voltage.

As a result, I and all the a_Q are functions of time. In most of the subsequent discussion, these will be referred to as $a_Q(t)$. Figure 1 illustrates this by an example. Both I and $a_1(t)$ have the same period as the LO waveform. In this example, moreover, the LO waveform is cosinusoidal; the bias term B in equation (3) is:

$$B = V_B + V_{AC} \cos \theta_{LO} \quad (10a)$$

where

- V_B is the DC bias voltage
- V_{AC} is the peak voltage of the Thevenin equivalent LO source voltage
- θ_{LO} has values from $-\pi$ to π and is the instantaneous local oscillator phase angle ($=2\pi f_{LO} t$).

Thus, B is shown to be periodic. Note also that

$$v_t - B = v_{RF} \quad (11)$$

where

v_{RF} is the input voltage waveform at the RF.

$R_b = 13 \text{ ohms}$
 $I_0 = 2 \text{ } \mu\text{amps}$
 $\alpha = 24.6$
 $R_s = R_T = 50 \text{ ohms}$
 $V_B = 3.0 \text{ volts}$
 $V_{AC} = 1.66 \text{ volts}$

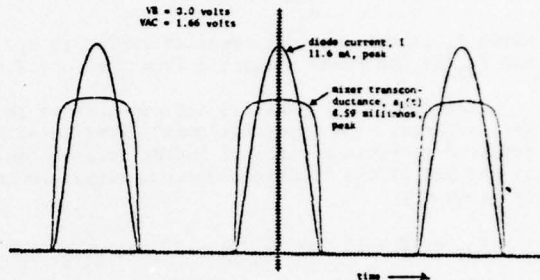


Figure 1. IN82A Diode Current and Mixer Transconductance Computed from Equations (5) and (9).

rewriting equation (3):

$$i = \sum_{Q=0}^7 a_Q(t) v_{RF}^Q \quad (12)$$

Because $a_Q(t)$ are periodic functions of time, each may be expanded in a truncated Fourier series.

$$a_Q(t) = \sum_{P=0}^{10} a_{P,Q} \cos(P2\pi f_{LO} t) \quad (13)$$

$$i = \sum_{P=0}^{10} \sum_{Q=0}^7 v_{RF}^Q a_{P,Q} \cos(P2\pi f_{LO} t) \quad (14)$$

First we see that the current has many frequency components. In general, only one will be of concern, the one appearing at the IF (i.e., f_{IF}). For example, let the IF = 3 MHz and the LO frequency (f_{LO}) be 35 MHz. Then any signal at a frequency such that:

$$f_{RF} = \frac{35P+3}{Q} \quad (15)$$

will result in a component at 3 MHz. Moreover, a signal at either 32 or 38 MHz is termed a desired (or image) frequency; these correspond to $P=Q=1$. Signal frequencies of 67 and 73 MHz will also result in 3 MHz responses ($P=2, Q=1$), and so forth.

Let the input signal, in any case, be given by:

$$v_{RF} = V_{RF} \cos 2\pi f_{RF} t \quad (16)$$

The peak current component at the IF is, from (14) and (16):

$$i_{P,Q} = \binom{10}{P} \binom{7}{Q} V_{RF}^Q a_{P,Q} \quad , P > 0 \quad (17)$$

ESD-TR-78-100

The above equation must now be related to the measured quantities. For the circuit of Figure 2, the following may be obtained.

$$P_L = 10 \log (R_L i_{P,Q}^2) + 27 \quad \text{dBm} \quad (18)$$

$$P_{AV} = 10 \log \frac{V_{RF}^2}{R_S} + 21 \quad \text{dBm} \quad (19)$$

where P_L is the spurious power delivered to R_L and P_{AV} is the power available from the source

The desired response is defined here as the $P=1, Q=1$ response. The input "on-tune" power level P_{OT} required to yield a given IF output level S (which is defined as the standard response output level) is given by:

$$P_{OT} = S - 10 \log (R_L R_S) - 20 \log a_{1,1} \quad \text{dBm} \quad (20)$$

The input available power level, at an RF frequency picked to result in a particular spurious (P,Q) response, called P_{spur} , may be related to P_{OT}

$$P_{spur} = 27 - 10 \log R_S + \left[P_{OT} + 10 \log R_S + 20 \log \left| \frac{a_{1,1}}{a_{P,Q}} \right| - 27 \right] / Q \quad (P > 0) \quad \text{dBm} \quad (21)$$

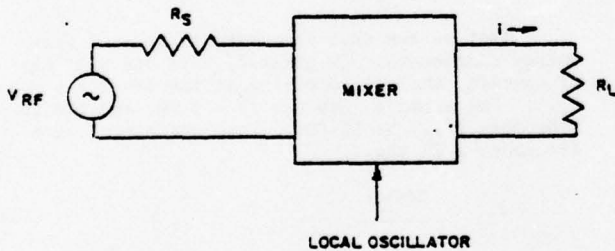


Figure 2. Mixer Circuit Diagram

Sample Output

A sample output sheet of the IMSPUR program is presented in Figure 3. The inputs are printed first.

On the next line it may be seen that the circuit, although extremely hard-driven is not very efficient. (Note that the desired input power is user supplied). Design features to achieve more efficient conversion have not been attempted. Techniques could include: faster LO rise time, trap filters at the LO frequency and RF to by-pass the load resistor (and thus increase the effective diode voltages at these frequencies) and matching the sources to the diode resistance, R_d , discussed below. Next are some calculated parameters of interest. The fundamental frequency local oscillator current estimated to be present in the load re-

Appendix C

sistance is printed, along with the second harmonic current. The relative levels suggest that the diode is being driven extremely hard. This is the appropriate condition. On the next line we have the RF circuit resistance. From equation (14) we see that this is $1/a_{1,1}$ ohms, the diode resistance at the desired RF must then be:

$$R_d = (1/a_{1,1}) - R_T \quad \text{ohms} \quad (22)$$

Finally, we have the matrix of input (available) power levels required to produce a standard IF response, in this case, -116.8 dBm.

```

THE NUMBER OF PROBLEMS SOLVED IS 2
THE NUMBER TRANSFORM INTERNAL STEPS IS 512
INPUTS ARE      ALF 20.0  BULK RECD 13.000MS  LEADAGE = .200-00LAMPERS-REVERSE
SOURCE SINUS   .2200V/15.00000  PWRN ACC 11.000 VOLTS
THE MAIN SOURCE RESISTANCE  50.000MS  LOAD RESISTANCE  50.000MS

USER SUPPLIED DESIRED IN OF  -99.2 DBM-GETS STANDARD RESP AT  -116.8 DBM
OSCILLATOR CURRENT FUND =  .270E-2 AMPS  2ND HARMONIC     .10-0E-2 AMPS
OF CIRCUIT AC RESISTANCES  200.0  OHMS

    001    002    003    004    005    006    007    *****
-100.0  -20.7  -10.0  -7.0  -1.7  .0  -1.2  PW  0  INPUT DBM
-99.0   -20.0  -10.0  -7.0  -1.7  0.0  -1.1  PW  1  INPUT DBM
-98.0   -20.0  -17.0  -9.0  -1.8  -0.0  -1.1  PW  2  INPUT DBM
-97.0   -20.0  -25.0  -10.0  -2.0  1.1  1.0  PW  3  INPUT DBM
-96.0   -27.0  -20.0  -12.0  -2.0  -1.5  .0  PW  4  INPUT DBM
-95.7   -27.0  -21.5  -12.0  -2.0  -0.7  .3  PW  5  INPUT DBM
-95.0   -20.0  -22.0  -12.0  -2.0  -0.3  .3  PW  6  INPUT DBM
-94.0   -27.0  -21.1  -10.0  -2.0  -0.5  -2.0  PW  7  INPUT DBM
-93.0   -25.0  -23.0  -13.0  -10.0  -0.0  -1.0  PW  8  INPUT DBM
-92.0   -27.0  -19.0  -12.0  -0.7  -7.1  -2.1  PW  9  INPUT DBM
-91.0   -27.0  -22.0  -12.0  -11.0  -0.0  -0.0  PW 10  INPUT DBM
    
```

Figure 3. IMSPUR Computer Program Sample Output.

Comparisons With Measured Data

Following are comparisons with measured data. It should be emphasized that the predictions were based solely on the DC characteristics of the diode and a linear circuit analysis. IMSPUR is not an empirical or statistical model based on spurious response or dynamic response measured data.

The measured data for a diode mixer test circuit are shown on TABLE 1(a) for an LO voltage (Thevenin equivalent) of 0.468v, peak. The corresponding IMSPUR predictions are shown in TABLE 1(b). Note that forty-two of the predicted values (i.e., well over half) differ by less than 1 dB from the measured values. The average difference is 1 dB. The standard deviation of the differences (or error, if you like) is 3.1 dB. For illustration, some of these data are shown on Figure 4.

A sensitivity analysis of the IMSPUR prediction accuracy was performed, as a function of input parameter values. The results are presented in TABLES 2(a) and 2(b). It is seen that the standard error is minimum when the values of i_1 and a arrived at through examination of the DC characteristics are employed.

One purpose of the measurements was to test for a need to include frequency dependent diode parameters such as junction capacitance. For this purpose refer to TABLE 3. In this table are the input signal frequencies which were applied in order to obtain each (P,Q) spurious response. There are two values for each P,Q combination; note the \pm signs of equation (15). The predictions (TABLE 1) associated with signal frequencies above 300 MHz are noticeably increasing in error. Although accuracies presently

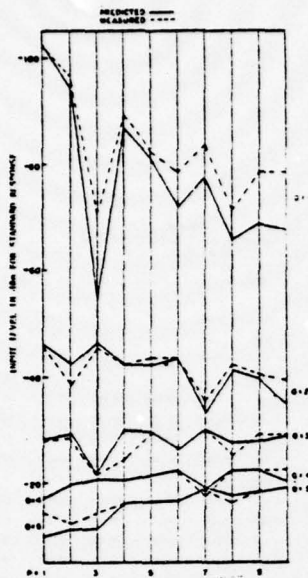


Figure 4. TABLE 1 Data Plotted for Comparison, Through Q=5.

obtainable are acceptable for many purposes in the UHF band, there seems a need for additional refinement here.

The measured data for a condition of an LO voltage (Thevenin equivalent) of 1.66v peak are shown on TABLE 4(a). The corresponding INSPUR predictions are on TABLE 4(b). The results are comparable although increased error is seen for Q=5, 6, and 7 and P=1 responses. Two possible explanations are: inability to handle input RF levels approaching the LO level and, second, undetected RF source harmonic leakage into the test circuit. In any case, the results are still reasonably accurate considering the one-hundred dB range of the responses.

CONCLUDING COMMENTS

While additional levels of complexity could have been employed in the INSPUR computer program, the test comparison results were excellent. One can expect to be within 3 dB of the mixer sensitivity to a given spurious frequency for 17 orders of non-linearity.

Additional features which could be added include consideration of the diode shunt resistance in the Taylor series expansion.

Reactive elements could also be included; note that model errors increased somewhat for frequencies above 300 MHz. The subject is covered in the RADIC report in more detail.

APPENDIX I

In the text, the periodic time-varying power-series coefficient $a_1(t)$ was derived. It was said that $a_1(t)$, when expanded in a Fourier series, yielded the constant coefficients $a_{p,1}$ for $p = 0, 1, 2, \dots$. Below the expressions for $a_Q(t)$ for $Q = 2, 3, 4, \dots, 7$ are presented. For convenience, these will revert back to the notation used previously, i.e., $a_1 = a_1(t)$.

In addition, define μ , such that

$$\mu = R_T a_1 - 1 \tag{I-1}$$

then we obtain:

$$a_2 = \alpha a_1 \mu^2 / 2 \tag{I-2}$$

$$a_3 = \alpha a_2 \mu^2 / 3 + 2\alpha R_T a_1 a_2 \mu / 5 \tag{I-3}$$

$$a_4 = \alpha a_3 \mu^2 / 4 + \alpha R_T (4R_T a_1 a_2^2 + 6a_1 a_3 \mu + 8a_2^2 \mu) / 12. \tag{I-4}$$

$$a_5 = \alpha a_4 \mu^2 / 5 + \alpha R_T (36 R_T a_1 a_2 a_3 + 24 R_T a_2^3 + 72 a_2 a_3 \mu + 24a_1 a_4 \mu) / 60, \tag{I-5}$$

$$a_6 = \alpha a_5 \mu^2 / 6 + \alpha R_T (432 R_T a_1 a_2^2 a_3 + 108 R_T a_1 a_3^2 + 192 R_T a_1 a_2 a_4 + 216a_3^2 \mu + 384a_2 a_4 \mu + 120a_1 a_5 \mu) / 360 \tag{I-6}$$

$$a_7 = \alpha a_6 \mu^2 / 7 + \alpha R_T (5240R_T a_1 a_2 a_3^2 + 2880 R_T a_2^2 a_4 + 1440 R_T a_1 a_3 a_4 + 1200 R_T a_1 a_2 a_5 + 2880a_3 a_4 \mu + 2400a_2 a_5 \mu + 720a_1 a_6 \mu) / 2520 \tag{I-7}$$

Each of these is a periodic time function of a periodic time function. The INSPUR computer program expands each $a_Q(t)$ in a Fourier series whose constant coefficients are $a_{p,Q}$, $p=0, 1, 2, \dots, 10$.

Acknowledgement

The work contained herein was performed under Contract No. F-19628-76-C0017 for the Department of Defense at the Electromagnetic Compatibility Analysis Center, Annapolis, Md. Measurements were performed by J. Walker of IITRI/ECAC.

References

1. Herishen, J. T., Diode Mixer Coefficients for Spurious Response Prediction, IEEE Transactions on EMC, Vol. EMC-10, No. 4, Dec. 1968.
2. Steiner, J. W., An Analysis of Radio Frequency in Interference Due To Mixer Intermodulation Products, IEEE Transactions on EMC, January, 1964.
3. Davenport and Root, Random Signals and Noise, McGraw-Hill, 1958.
4. Schemel, R., A Method of Calculating the Intermodulation Products in The--Etc. Shape Technical Center, STC-TM-288, June 1971.
5. Fuenzalida, Shimbo, and Cook, Time Domain Analysis of Intermodulation Effects Caused by Nonlinear Amplifiers, COMSAT Technical Review Vol. 3, No. 1, Spring, 1973.
6. Terman, F. E., Electronic and Radio Engineering, McGraw-Hill, Fourth Edition, 1955, pages 573 to 575.

7. Nonlinear System Modeling and Analysis with Applications to Communications Receivers, RADC-TR-73-178, June 1973.

8. ECAC LAB Memo # 7769, May, 1977.

TABLE 1a
MEASURED SPURIOUS RESPONSE VALUES FOR SINGLE ENDED
INTELA MIXER WITH $F_{LO} = 0$ dBm (VALUES IN dBm)
($F_{LO} = -2.6$ dBm with diode bypassed.)

P →	1	2	3	4	5	6	7	8	9	10
Q ↓										
1	-102.4	-96.4	-79.4	-69.4	-62.4	-78.4	-83.4	-71.4	-78.4	-78.4
2	-45.4	-38.4	-45.4	-42.4	-43.4	-35.4	-42.4	-40.4	-39.4	-39.4
3	-28.4	-28.4	-23.4	-26.4	-29.4	-26.4	-30.4	-23.4	-29.4	-29.4
4	-17.4	-19.4	-21.4	-20.4	-21.4	-22.4	-17.4	-22.4	-22.4	-22.4
5	-16.4	-12.4	-14.4	-16.4	-16.4	-16.4	-18.4	-16.4	-18.4	-18.4
6	-11.4	-11.4	-9.4	-11.4	-13.4	-14.4	-12.4	-15.4	-14.4	-15.4
7	-10.4	-9.4	-8.4	-9.4	-9.4	-11.4	-12.4	-11.4	-12.4	-13.4

TABLE 1b
PREDICTED SPURIOUS RESPONSE VALUES FOR SINGLE ENDED
INTELA MIXER WITH $F_{LO} = 0$ dBm

P →	1	2	3	4	5	6	7	8	9	10
Q ↓										
1	-102.4	-95.4	-84.5	-66.7	-81.0	-71.5	-77.2	-65.7	-66.4	-67.3
2	-46.1	-42.4	-46.1	-42.1	-42.3	-43.1	-32.7	-41.1	-39.3	-35.0
3	-28.3	-29.3	-21.7	-29.9	-29.6	-26.1	-29.9	-27.6	-27.9	-28.6
4	-16.9	-19.7	-21.4	-20.1	-21.7	-22.8	-18.6	-22.8	-22.6	-20.2
5	-10.1	-11.1	-11.1	-16.8	-16.8	-16.4	-18.5	-17.4	-18.2	-19.0
6	-9.5	-9.2	-8.9	-11.8	-13.8	-14.4	-11.7	-15.5	-15.5	-14.7
7	-8.5	-8.6	-8.7	-8.9	-8.6	-11.7	-12.6	-11.1	-13.3	-13.8

TABLE 2(a)
MEAN ERROR IN dB

F_{LO} (dBm) \ α	10	20	24.8	30	40
1.0	0.9				
2.0	3.9	2.6	1.0	0.5	1.4
10.0	1.3				
100.0	1.4				

TABLE 2(b)
STANDARD ERROR IN dB

F_{LO} (dBm) \ α	10	20	24.8	30	40
1.0	5.5				
2.0	14.4	5.8	3.1	4.3	6.1
10.0	4.7				
100.0	4.7				

TABLE 3
MATRIX OF SPURIOUS RESPONSE FREQUENCIES FOR P=1-10
 $Q = 1-10$ WITH $F_{LO} = 15$ MHz AND $F_{IF} = 3$ MHz

P →	1	2	3	4	5	6	7	8	9	10
Q ↓										
1	58	73	104	143	178	213	248	283	318	353
2	32	67	102	137	172	207	242	277	312	347
3	19	36,500	54,000	71,500	89,000	106,500	124,000	141,500	159,000	176,500
4	16	33,500	51,000	68,500	86,000	103,500	121,000	138,500	156,000	173,500
5	12,667	24,334	36,000	47,667	59,333	71,000	82,667	94,333	106,000	117,667
6	10,667	22,334	34,000	45,667	57,333	69,000	80,667	92,333	104,000	115,667
7	9,500	18,750	27,000	35,750	44,500	53,250	62,000	70,750	79,500	88,250
8	8,000	16,750	25,500	34,250	43,000	51,750	60,500	69,250	78,000	86,750
9	7,600	14,800	21,600	28,600	35,600	42,600	49,600	56,600	63,600	70,600
10	6,400	13,400	20,400	27,400	34,400	41,400	48,400	55,400	62,400	69,400
11	6,334	12,167	18,000	23,834	29,667	35,500	41,333	47,167	53,000	58,833
12	5,334	11,167	17,000	21,833	26,667	31,500	36,333	41,167	46,000	50,833
13	5,429	10,429	15,429	20,429	25,429	30,429	35,429	40,429	45,429	50,429
14	4,571	9,571	14,571	19,571	24,571	29,571	34,571	39,571	44,571	49,571

TABLE 4a
MEASURED SPURIOUS RESPONSE VALUES FOR SINGLE ENDED
INTELA MIXER WITH $F_{LO} = -10$ dBm
($F_{LO} = -8.8$ dBm with diode bypassed.)

P →	1	2	3	4	5	6	7	8	9	10
Q ↓										
1	-89.2	-83.2	-69.2	-53.2	-63.2	-80.2	-81.2	-77.2	-82.2	-82.2
2	-31.2	-36.2	-34.2	-37.2	-34.2	-36.2	-36.2	-36.2	-37.2	-35.2
3	-14.2	-16.2	-18.2	-17.2	-20.2	-19.2	-20.2	-20.2	-19.2	-21.2
4	-7.2	-5.2	-8.2	-9.2	-10.2	-11.2	-14.2	-15.2	-11.2	-12.2
5	-10.2	-7.2	-5.2	-2.2	-4.2	-5.2	-7.2	-9.2	-10.2	-7.2
6	-4.2	-2.2	-5.2	-3.2	-0.2	-2.2	-2.2	-3.2	-4.2	-5.2
7	-7.2	-5.2	-2.2	-0.3	+1.8	+1.8	+1.8	-0.2	-1.2	-2.2

TABLE 4b
PREDICTED SPURIOUS RESPONSE VALUES FOR SINGLE ENDED
INTELA MIXER WITH $F_{LO} = -10$ dBm

P →	1	2	3	4	5	6	7	8	9	10
Q ↓										
1	-89.2	-84.2	-67.9	-52.2	-60.7	-80.2	-73.6	-78.2	-84.3	-75.9
2	-32.8	-39.0	-36.2	-37.9	-34.4	-36.2	-37.9	-33.5	-37.9	-27.6
3	-19.6	-17.0	-21.0	-20.6	-21.5	-22.4	-21.1	-23.4	-19.4	-23.9
4	-5.6	-9.8	-9.6	-12.5	-13.0	-13.5	-14.8	-13.4	-15.9	-11.7
5	-2.3	-1.0	-5.0	-5.4	-7.6	-8.4	-8.6	-10.2	-8.7	-11.4
6	+1.7	-0.8	+1.1	-1.5	-2.7	-4.3	-3.5	-5.4	-7.1	-5.4
7	+5.3	0	+1.8	-0.2	+0.5	+0.5	-2.7	-3.2	-3.1	-4.8

APPENDIX D
CALCULATING DIODE PARAMETERS

TABLE D-1 presents dc diode measured data for the diode used in the mixer of APPENDIX C. The measurement circuit is shown in Figure D-1. For each dc source voltage level, the voltages at points (1) and (2) were measured. The diode voltage is the difference between these two data. The diode current is the voltage at point (2) divided by the load resistance of 50 ohms.

Examination of the measured data clearly indicates a *reverse leakage current* of 2 microamperes. In addition, a diode *shunt resistance* of 125 kilohms is indicated; note that, for reverse voltages greater than about $\frac{1}{2}$ volt, the reverse voltage has a slope of about 125 k Ω . We now have two of the four diode model parameters. By submitting these two parameters and the measured data for forward voltages to the computer program discussed below, the other two diode parameters are obtained.

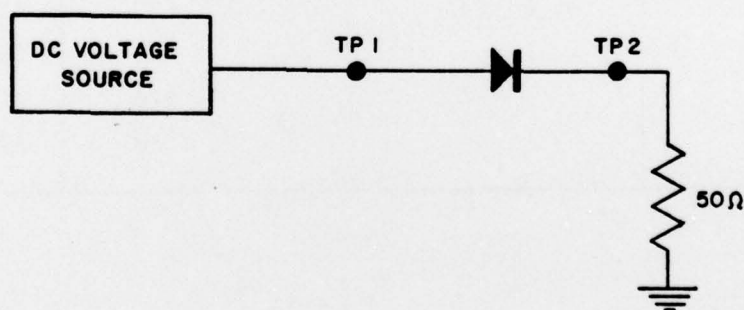


Figure D-1. Measurement circuit for dc characteristic of diode.

TABLE D-1
MEASURED 1N82A DIODE DC CHARACTERISTIC

REVERSE		FORWARD	
V (mV)	I (μ A)	V (mV)	I (μ A)
-3988	-263	249	2
-2997	- 67	497	6
-1999	- 23	992	16
-1499	- 12	189	231
-1000	- 6	256	926
- 800	- 6	303	2040
- 600	- 4	341	3340
- 500	- 2	372	4800
- 400	- 2	404	6320
- 300	- 2	436	7660
- 200	- 2	465	9150
- 100	- 2	480	10940
- 50	- 1	620	18520
		750	26310
		970	42730
		1180	59360

Figure D-2 provides the reader with a FORTRAN-V listing of DCPAR, a computer program that identifies appropriate values of the diode dc parameters α (alpha) and R_b (bulk resistance). The user supplies the following data. See above for example acquisition of the first two.

1. Diode reverse leakage current, i_0
2. Diode model shunt (parallel) resistance, R_{SH} (results are generally very insensitive to $R_{SH} > 100 \text{ k}\Omega$.)
3. Pairs of diode dc current and forward diode voltages, I and V data, respectively
4. The number (NVI) of current and voltage data pairs.

A sample output is provided in Figure D-3. The first column is the value of R_b selected. The second column is the range of calculated alpha values calculated from the NVI data pairs of current-voltage. The next column is the average value of the alphas calculated from the ND data pairs assuming the same value of R_b . The last column is the standard deviation of alpha values. Since alpha and R_b are assumed independent of applied voltage, the value of R_b that yields the most constant value of alpha for the entire set of submitted data pairs is seen to be $R_b = 13 \text{ ohms}$ and $\alpha = 24.8 \text{ inverse volts}$.

```

C
C   FIND ALPHA
   DIMENSION V(100),C(100),ALPHA(100)
   READ(5,100) NVI,RSH,CL
100  FORMAT(I2,2F8.6)
   DO 1 I=1,NVI
   READ(5,105) V(I),C(I)
105  FORMAT(2F8.6)
   1  CONTINUE
   RS=.1
   WRITE(6,110)
110  FORMAT(16X,'RS',15X,'MAX-MIN',15X,
*AVE',15X,'SIGMA',/,16X,2(1H-),
*15X,7(1H-),15X,3(1H-),15X,5(1H-))
500  A=-1000.
   B=1000.
   TOTAL=0.
   DO 10 I=1,NVI
   ALPHA(I)=ALOG(C(I)/CL-V(I)/(CL*RSH)+1)
* / (V(I)*(1+RS/RSH)-C(I)*RS)
   A=AMAX1(A,ALPHA(I))
   B=AMIN1(B,ALPHA(I))
   TOTAL=ALPHA(I)+TOTAL
   10  CONTINUE
   DIFF=A-B
   AVE=TOTAL/NVI
   SIGSQ=0.
   DO 15 J=1,NVI
15  SIGSQ=SIGSQ+(ALPHA(J)-AVE)**2/NVI
   SIGMA=SQRT(SIGSQ)
   WRITE(6,120) RS,DIFF,AVE,SIGMA
120  FORMAT(10X,E14.7,6X,E14.7,6X,E14.7,
*6X,E14.7)
   IF(RS-.1) 50,50,55
   50  RS=RS+.4
   GO TO 500
55  IF(RS-20.000000) 60,75,75
   60  RS=RS+.5
   GO TO 500
   75  END

```

Figure D-2. DCPAR listing.

RS --	MAX-MIN -----	AVE ---	SIGMA -----
.1000000+00	.1809652+02	.1941942+02	.5254997+01
.5000000+00	.1791671+02	.1951967+02	.5192572+01
.1000000+01	.1768116+02	.1964809+02	.5111424+01
.1500000+01	.1743272+02	.1978015+02	.5026580+01
.2000000+01	.1717030+02	.1991604+02	.4937762+01
.2500000+01	.1689269+02	.2005598+02	.4844666+01
.3000000+01	.1659855+02	.2020021+02	.4746956+01
.3500000+01	.1628636+02	.2034900+02	.4644259+01
.4000000+01	.1595443+02	.2050264+02	.4536159+01
.4500000+01	.1560081+02	.2066144+02	.4422195+01
.5000000+01	.1522333+02	.2082576+02	.4301852+01
.5500000+01	.1481949+02	.2099598+02	.4174554+01
.6000000+01	.1438646+02	.2117254+02	.4039659+01
.6500000+01	.1392095+02	.2135592+02	.3896446+01
.7000000+01	.1341919+02	.2154667+02	.3744109+01
.7500000+01	.1287679+02	.2174539+02	.3581750+01
.8000000+01	.1228860+02	.2195279+02	.3408372+01
.8500000+01	.1164861+02	.2216966+02	.3222883+01
.9000000+01	.1094966+02	.2239691+02	.3024118+01
.9500000+01	.1018325+02	.2263559+02	.2810888+01
.1000000+02	.9339121+01	.2288694+02	.2582118+01
.1050000+02	.8404858+01	.2315239+02	.2337147+01
.1100000+02	.7365237+01	.2343364+02	.2076433+01
.1150000+02	.6201403+01	.2373275+02	.1803233+01
.1200000+02	.5169052+01	.2405219+02	.1527848+01
.1250000+02	.5168901+01	.2439501+02	.1278355+01
.1300000+02	.5168750+01	<u>.2476497+02</u>	a .1122547+01
.1350000+02	.5448569+01	.2516688+02	.1172002+01
.1400000+02	.7758108+01	.2560693+02	.1489731+01
.1450000+02	.1049709+02	.2609327+02	.2043900+01
.1500000+02	.1379747+02	.2663702+02	.2803228+01
.1550000+02	.1785142+02	.2725370+02	.3778534+01
.1600000+02	.2295012+02	.2796596+02	.5021186+01
.1650000+02	.2955698+02	.2880852+02	.6630619+01
.1700000+02	.3845698+02	.2983796+02	.8784896+01
.1750000+02	.5109424+02	.3115473+02	.1181830+02
.1800000+02	.7044768+02	.3295916+02	.1642832+02
.1850000+02	.1038076+03	.3572732+02	.2433919+02
.1900000+02	.1749981+03	.4097903+02	.4124353+02
.1950000+02	.4326199+03	.5805095+02	.1029673+03
.2000000+02	.1555083+04	-.6092563+02	.3638061+03
.2050000+02	.3865443+03	.1496420+02	.7871100+02

^aBest α is 24.8 volts⁻¹.

Figure D-3. DCPAR output.

The method employed in the program makes use of the following equations.

$$i_D = i_0 \left[e^{\alpha v'_D} - 1 \right], \quad \text{amperes (D-1)}$$

$$V'_D = V - i_D R_b, \quad \text{volts (D-2)}$$

$$I = i_D + V/R_{SH}, \quad \text{amperes (D-3)}$$

Given values for R_{SH} , i_0 and R_b , then a value of alpha for each pair of i and v data is computed. When the entire set of NVI pairs have been exhausted, the spread, average, and standard deviation of resulting alphas is printed. The value of R_b is then changed and the process is repeated. The increments and range of R_b are fixed in the program. DCPAR input formats are as follows.

CARD 1

COLUMNS	FORMAT	DESCRIPTION
1-2	INT ^a	NUMBER OF CURRENT AND VOLTAGE DATA PAIRS, NVI
3-11	FL.PT. ^b	DIODE MODEL SHUNT RESISTANCE, R_{SH} (OHMS)
12-20	FL.PT.	DIODE REVERSE LEAKAGE CURRENT, i_0 (AMPS)

CURRENT AND VOLTAGE DATA CARDS

COLUMNS	FORMAT	DESCRIPTION
1-8	FL.PT.	DIODE VOLTAGE (VOLTS)
9-16	FL.PT.	DIODE CURRENT (AMPS)

^aInteger.

^bFL.PT.- Floating point.

APPENDIX E

NUMERICAL SOLUTION FOR DOUBLE-BALANCED-DIODE MIXER CURRENTS

The circuit diagram of the double-balanced-diode mixer (DBDM) is shown in Figure 6, and consists of four independent current loops or meshes. In the computer program, the applied local oscillator is a known quantity and the current through each of the four diodes must be calculated from Equation 16.

If the four diodes were each replaced with a linear resistor, the problem would become a trivial linear circuit problem that could be easily solved in closed form with simple expressions for each of the unknown currents; these currents could be evaluated for each possible applied local oscillator voltage. However, the presence of the highly nonlinear diodes demands an alternative approach.

The procedure employed is a "relaxation" method in which initial assumptions are made for each of the four diode currents. The value of one of the currents is then "relaxed" and the current recomputed with the other three currents regarded as fixed at their presently assumed values. In fact, each of the other three diodes is regarded as a current generator supplying the assumed current. Under these conditions, the equivalent circuit may be reduced to a single mesh containing a diode, an equivalent resistance, and an equivalent voltage source. The problem then becomes one of solving the transcendental Equation E-1 for the unknown current i_j :

$$i_j = i_{0,j} \left[\frac{\alpha_j (v_j - R_j i_j)}{e^{j(v_j - R_j i_j)} - 1} \right] \quad (E-1)$$

In Equation E-1, the terms $i_{0,j}$ and α_j are the Ebers-Moll parameters of the J^{th} diode; R_j is the total resistance of the single mesh equivalent circuit corresponding to diode j ; and V_j is the equivalent circuit voltage.

Equation E-1 is the Ebers-Moll diode model (the shunt resistor R_{SH} is ignored here) and may be solved for the unknown current by means of an iterative procedure. To insure rapid convergence of the procedure by which the diode current is determined, one of two alternative formulations is selected based on the sign of the voltage V_j . In particular, for $V_j \geq 0$, the Newton-Raphson method is used to calculate the root of $G_1(i_j)$:

$$G_1(i_j) = i_{0,j} \left\{ \exp \left[\alpha_j (v_j - R_j i_j) \right] - 1 \right\} - i_j = 0 \quad (\text{E-2})$$

while for $V_j < 0$ the root of $G_2(i_j)$ is calculated using:

$$G_2(i_j) = \alpha_j (v_j - R_j i_j) - \ln (i_j / i_{0,j} + 1) = 0 \quad (\text{E-3})$$

After each of the diode currents is recomputed in this fashion it is regarded as a known quantity while each of the other three currents is "relaxed" in turn and subsequently recomputed. The entire process of computing all four currents is repeated until changes in successive estimates of each of the currents are all less than the precision required of the computation, i.e. 10^{-9} amperes in the actual program. Experience with this procedure showed that in general the process converged within 10^{-9} amperes within three or fewer iterations over the set of four diodes.

APPENDIX F
THE C^Q EXPRESSIONS

$$C^1 = \begin{bmatrix} -k_1 \alpha_1 J_1 \\ -k_2 \alpha_2 J_2 \\ +k_1 \alpha_3 J_3 \\ +k_2 \alpha_4 J_4 \end{bmatrix}$$

$$C^2 = \begin{bmatrix} -\frac{1}{J_1} \left(\frac{\partial i_1}{\partial e_s} \right)^2 \\ -\frac{1}{J_2} \left(\frac{\partial i_2}{\partial e_s} \right)^2 \\ -\frac{1}{J_3} \left(\frac{\partial i_3}{\partial e_s} \right)^2 \\ -\frac{1}{J_4} \left(\frac{\partial i_4}{\partial e_s} \right)^2 \end{bmatrix}$$

$$C^3 = \begin{bmatrix} -\frac{3}{J_1} \frac{\partial i_1}{\partial e_s} \frac{\partial^2 i_1}{\partial e_s^2} + \frac{2}{J_1^2} \left(\frac{\partial i_1}{\partial e_s} \right)^3 \\ -\frac{3}{J_2} \frac{\partial i_2}{\partial e_s} \frac{\partial^2 i_2}{\partial e_s^2} + \frac{2}{J_2^2} \left(\frac{\partial i_2}{\partial e_s} \right)^3 \\ -\frac{3}{J_3} \frac{\partial i_3}{\partial e_s} \frac{\partial^2 i_3}{\partial e_s^2} + \frac{2}{J_3^2} \left(\frac{\partial i_3}{\partial e_s} \right)^3 \\ -\frac{3}{J_4} \frac{\partial i_4}{\partial e_s} \frac{\partial^2 i_4}{\partial e_s^2} + \frac{2}{J_4^2} \left(\frac{\partial i_4}{\partial e_s} \right)^3 \end{bmatrix}$$

Noting similarities in the matrix terms, we may also write the members of C^3 as:

$$C_r^3 = -\frac{3}{J_r} \frac{\partial i_r}{\partial e_s} \frac{\partial^2 i_r}{\partial e_s^2} + \frac{2}{J_r^2} \left(\frac{\partial i_r}{\partial e_s} \right)^3 \quad r = 1, 2, 3, 4$$

Carrying on with the new notation:

$$C_r^4 = -\frac{4}{J_r} \frac{\partial i_r}{\partial e_s} \frac{\partial^3 i_r}{\partial e_s^3} + \frac{12}{J_r^2} \left(\frac{\partial i_r}{\partial e_s} \right)^2 \frac{\partial^2 i_r}{\partial e_s^2} - \frac{3}{J_r} \left(\frac{\partial^2 i_r}{\partial e_s^2} \right)^2 - \frac{6}{J_r^3} \left(\frac{\partial i_r}{\partial e_s} \right)^4 \quad r = 1, 2, 3, 4$$

$$C_r^5 = -\frac{5}{J_r} \frac{\partial i_r}{\partial e_s} \frac{\partial^4 i_r}{\partial e_s^4} + \frac{20}{J_r^2} \left(\frac{\partial i_r}{\partial e_s} \right)^2 \frac{\partial^3 i_r}{\partial e_s^3} - \frac{10}{J_r} \frac{\partial^2 i_r}{\partial e_s^2} \frac{\partial^3 i_r}{\partial e_s^3} - \frac{60}{J_r^3} \left(\frac{\partial i_r}{\partial e_s} \right)^3 \frac{\partial^2 i_r}{\partial e_s^2} + \frac{30}{J_r^2} \frac{\partial i_r}{\partial e_s} \left(\frac{\partial^2 i_r}{\partial e_s^2} \right)^2 + \frac{24}{J_r^4} \left(\frac{\partial i_r}{\partial e_s} \right)^5 \quad r = 1, 2, 3, 4$$

$$C_r^6 = -\frac{6}{J_r} \frac{\partial i_r}{\partial e_s} \frac{\partial^5 i_r}{\partial e_s^5} + \frac{30}{J_r^2} \left(\frac{\partial i_r}{\partial e_s} \right)^2 \frac{\partial^4 i_r}{\partial e_s^4} - \frac{15}{J_r} \frac{\partial^2 i_r}{\partial e_s^2} \frac{\partial^4 i_r}{\partial e_s^4} - \frac{120}{J_r^3} \left(\frac{\partial i_r}{\partial e_s} \right)^3 \frac{\partial^3 i_r}{\partial e_s^3}$$

$$\begin{aligned}
& + \frac{120}{J_r^2} \frac{\partial i_r}{\partial e_s} \frac{\partial^2 i_r}{\partial e_s^2} \frac{\partial^3 i_r}{\partial e_s^3} - \frac{10}{J_r} \left(\frac{\partial^3 i_r}{\partial e_s^3} \right)^2 \\
& + \frac{360}{J_r^4} \left(\frac{\partial i_r}{\partial e_s} \right)^4 \frac{\partial^2 i_r}{\partial e_s^2} - \frac{270}{J_r^3} \left(\frac{\partial i_r}{\partial e_s} \right)^2 \left(\frac{\partial^2 i_r}{\partial e_s^2} \right)^2 \\
& + \frac{30}{J_r^2} \left(\frac{\partial^2 i_r}{\partial e_s^2} \right)^3 - \frac{120}{J_r^5} \left(\frac{\partial i_r}{\partial e_s} \right)^6 \quad r = 1, 2, 3, 4
\end{aligned}$$

$$\begin{aligned}
C_r^7 = & - \frac{7}{J_r} \frac{\partial i_r}{\partial e_s} \frac{\partial^6 i_r}{\partial e_s^6} + \frac{62}{J_r^2} \left(\frac{\partial i_r}{\partial e_s} \right)^2 \frac{\partial^5 i_r}{\partial e_s^5} \\
& - \frac{21}{J_r} \frac{\partial^2 i_r}{\partial e_s^2} \frac{\partial^5 i_r}{\partial e_s^5} - \frac{270}{J_r^3} \left(\frac{\partial i_r}{\partial e_s} \right)^3 \frac{\partial^4 i_r}{\partial e_s^4} \\
& + \frac{250}{J_r^2} \frac{\partial i_r}{\partial e_s} \frac{\partial^2 i_r}{\partial e_s^2} \frac{\partial^4 i_r}{\partial e_s^4} - \frac{35}{J_r} \frac{\partial^3 i_r}{\partial e_s^3} \frac{\partial^4 i_r}{\partial e_s^4} \\
& + \frac{840}{J_r^4} \left(\frac{\partial i_r}{\partial e_s} \right)^4 \frac{\partial^3 i_r}{\partial e_s^3} - \frac{1,260}{J_r^3} \left(\frac{\partial i_r}{\partial e_s} \right)^2 \frac{\partial^2 i_r}{\partial e_s^2} \frac{\partial^3 i_r}{\partial e_s^3} \\
& + \frac{210}{J_r^2} \left(\frac{\partial^2 i_r}{\partial e_s^2} \right)^2 \frac{\partial^3 i_r}{\partial e_s^3} + \frac{140}{J_r^2} \frac{\partial i_r}{\partial e_s} \left(\frac{\partial^3 i_r}{\partial e_s^3} \right)^2 \\
& - \frac{2520}{J_r^5} \left(\frac{\partial i_r}{\partial e_s} \right)^5 \frac{\partial^2 i_r}{\partial e_s^2} + \frac{2,520}{J_r^4} \left(\frac{\partial i_r}{\partial e_s} \right)^3 \left(\frac{\partial^2 i_r}{\partial e_s^2} \right)^2 \\
& - \frac{630}{J_r^3} \frac{\partial i_r}{\partial e_s} \left(\frac{\partial^2 i_r}{\partial e_s^2} \right)^3 + \frac{720}{J_r^6} \left(\frac{\partial i_r}{\partial e_s} \right)^7 \quad r = 1, 2, 3, 4
\end{aligned}$$

Note that the units of C^Q are that of inverse volts times current raised to the Q th power (i^Q/v).

APPENDIX G

POWER SERIES DIVERGENCE FOR VACUUM TUBES

It is shown that the power series for vacuum tube amplifiers and mixers diverge in situations of interest. A general representation of a tube characteristic (Chapter 6 of Reference 3) is expanded in a power series. The ratio test for absolute convergence is applied, and the resulting expression is discussed.

The tube characteristic is calculated using:

$$i_p = e^{3/2} \quad (G-1)$$

where

i_p = plate current

e = an equivalent plate to cathode voltage, including the effects of the perveance, grid voltages, and amplification factor, as applicable.

From Equation 2, a general expression for the n^{th} order power series coefficient is given by Equation G-2:

$$a_n = \frac{3(-1)^n (2n-5)! I_p}{n! (n-3)! 2^{2n-3} E^n} \quad n \geq 3 \quad (G-2)$$

where

I_p = quiescent or dc plate current

E = quiescent or dc equivalent plate to cathode voltage.

The ratio test is applied by finding the limit as $n \rightarrow \infty$ of the absolute value of the ratio of the $(n+1)$ th term to the preceding term. If the limit exceeds unity, the series diverges.¹² Define this limit as r_t , then using this and Equation G-2:

$$r_t = \lim_{n \rightarrow \infty} \frac{a_{n+1} (v_{RF})^{n+1}}{a_n (v_{RF})^n} = \frac{v_{RF}}{E} \quad (G-3)$$

where

v_{RF} = the ac signal voltage.

As an example, the expression for E for a triode is given using:

$$E = E_c + \frac{E_b}{\mu} \quad (G-4)$$

where

E_c = control grid to cathode bias voltage

E_b = plate to cathode voltage

μ = plate amplification factor.

Values such as $E_b = 100$ and $\mu = 40$ are common even in amplifiers. Typically, E_c may range from -1 to -4 volts. Therefore, the value of E can be quite small. Consequently, the series can have a very small region of convergence.

¹²Sherwood and Taylor, *Calculus*, Prentice-Hall Inc., 3rd Ed., New York, NY, April 1954.

**DISTRIBUTION LIST FOR
ANALYSIS OF RECEIVER MIXERS
ESD-TR-78-100**

<u>DoD AND OTHERS</u>	<u>No. of Copies</u>	<u>NAVY (Continued)</u>	<u>No. of Copies</u>
Defense Documentation Center Cameron Station Alexandria, VA 22314	12	Dr. Peter Li Naval Ocean Systems Center San Diego, CA 92152	1
Director Defense Communications Agency Attn: Code 404A Washington, DC 20305	1	Dr. R. Adler Naval Postgraduate School Monterey, CA 93940	1
Director National Security Agency Attn: W36/Mr. V. McConnell Ft. George G. Meade, MD 20755	2	<u>MARINE CORPS</u> Director, Development Center Marine Corps Development and Education Command (Attn: CCC Div) Quantico, VA 22134	5
Department of Transportation Federal Aviation Administration Attn: ARD-62 2100 Second St., S.W. Washington, DC 20591	1	Director Communication Officers School Education Center, MCDEC Quantico, VA 22134	5
National Aeronautics & Space Administration Goddard Space Flight Center Attn: Code 801/Jim Scott Greenbelt, MD 20771	1	Commanding Officer Marine Corps Tactical Systems Support Activity Camp Pendleton, CA 92055	3
Chairman, MCEB (Room 1E-841) Pentagon Washington, DC 20301	1	Commander Naval Ocean Systems Center (Marine Corps Liaison Office) San Diego, CA 92152	2
<u>NAVY</u>		<u>ARMY</u>	
Commander (ELEX-095/Roney) Naval Electronic Systems Command Washington, DC 20360	1	CDR, USADARCOM Attn: DRCDE-DE (Mr. James Bender) 5001 Eisenhower Avenue Alexandria, VA 22333	1
Commander (ELEX-51024/Neill) Naval Electronic Systems Command Washington, DC 20360	1	CDR, USACORADCOM Attn: DRSEL-RD-TS-F (R. Tallman) Fort Monmouth, NJ 07703	1
Commander (AIR-52026) Naval Air Systems Command Washington, DC 20361	1	CDR, USACORADCOM Attn: DRDCO-COM-RY-5 (W. Kesselman) Fort Monmouth, NJ 07703	1
Commander (Code 6174D/Prout) Naval Ship Engineering Center Washington, DC 20362	1	CDR, USAMIRADCOM Attn: DRDMI-TE (D. Smith) Redstone Arsenal, AL 35807	1
Director Navy Electromagnetic Spectrum Center Attn: A. Rossmiller Naval Communication Unit Washington Washington, DC 20390	1	CDR, USACEEIA Attn: CCC-EMEO-ECD (Mr. B. Allen) Fort Huachuca, AZ 85613	1
Commanding Officer Naval Avionics Facility Attn: D. Fassburg 21st and Arlington Ave. Indianapolis, IN 46218	1	CDR, DCEC Attn: Code 430 Reston, VA 22090	1
		Director, Signal Warfare Lab Attn: IATEL-ZS (A. Casey) Arlington Hall Station Arlington, VA 22212	1